NASA TECHNICAL NOTE

NASA TN D-2054

NASA TN D-2054

EFFECT OF CONTROLLED SURFACE ROUGHNESS ON BOUNDARY-LAYER TRANSITION AND HEAT TRANSFER AT MACH NUMBERS OF 4.8 AND 6.0

by Paul F. Holloway and James R. Sterrett

Langley Research Center
Langley Station, Hampton, Va.

NATIONAL AERONAUTICS AND SPACE ADMINISTRATION • WASHINGTON, D. C. • APRIL 1964

EFFECT OF CONTROLLED SURFACE ROUGHNESS ON BOUNDARY-LAYER TRANSITION AND HEAT TRANSFER AT MACH NUMBERS OF 4.8 AND 6.0

By Paul F. Holloway and James R. Sterrett

Langley Research Center
Langley Station, Hampton, Va.

NATIONAL AERONAUTICS AND SPACE ADMINISTRATION

For sale by the Office of Technical Services, Department of Commerce,
Washington, D.C. 20230 -- Price $1.25

EFFECT OF CONTROLLED SURFACE ROUGHNESS ON BOUNDARY-LAYER TRANSITION AND HEAT TRANSFER AT MACH NUMBERS OF 4.8 AND 6.0

By Paul F. Holloway and James R. Sterrett

SUMMARY

An investigation has been conducted at a free-stream Mach number of 6.0 to determine the effects of controlled three-dimensional surface roughness (spheres) on boundary-layer transition and heat transfer. Experimental data are presented for a sharp-leading-edge two-dimensional flat-plate model over a local unit Reynolds number range of 1.2×10^6 to 8.2×10^6 per foot based on a local Mach number of 6.0 and 9.8×10^6 to 13.9×10^6 per foot based on a local Mach number of 4.8.

The Reynolds number for natural transition has been found to increase markedly with increasing Mach number above a Mach number of approximately 3.7. It was found that surface roughness of height less than the boundary-layer thickness can delay transition. The critical roughness Reynolds numbers determined experimentally in this investigation are larger than those found at lower supersonic Mach numbers. Roughness heights of approximately twice the calculated boundary-layer thickness at the roughness position were required to trip the boundary layer completely. Calculations of the heat-transfer distributions based on simple flat-plate theory are shown to agree reasonably well with the experimental results.

INTRODUCTION

The nature of boundary-layer transition and its effect on associated problem areas such as surface heat-transfer rates and aerodynamic characteristics has been the subject of many studies, yet there is still much to be learned about the phenomena. The data and theories on boundary-layer transition currently available for higher supersonic and hypersonic Mach numbers are limited at best and contain a great deal of scatter. Indeed, the designer of a high-speed configuration finds that it is difficult to evaluate the meaning of the available contradictory experimental and theoretical results.

One of the most important factors affecting the transition of the boundary layer from laminar to turbulent is the condition of the body surface. Surface irregularities such as expansion slots envisioned as necessary in winged reentry

vehicles (for example, the X-20), connecting rivets, or distortions due to high-temperature buckling of the skin material may well be prominent factors in determining the nature of the local boundary layer. Since it is possible that surface irregularities may cause boundary-layer transition, the designer of winged reentry configurations must be able to estimate the extent to which these irregularities may affect the location and length of transition and, in turn, the consequential effect on the surface heat-transfer rates.

Surface condition is also of importance from the experimental point of view since roughness may be utilized as a boundary-layer trip in wind-tunnel or free-flight tests. A guide is needed for determining the size of roughness required at high supersonic and hypersonic Mach numbers to obtain fully developed turbulent boundary layers which will duplicate full-scale conditions.

Considerable study has been devoted to boundary-layer transition and the factors affecting transition at subsonic and supersonic speeds. (See, for example, refs. 1 to 7.) In addition, recent work on the effects of surface distortions on the heat transfer to a wing at hypersonic speeds has been published in reference 8.

The purpose of this report is to present the results of an experimental study of the effects of one type of surface distortion of importance, controlled surface roughness (spheres), on boundary-layer transition and surface heat-transfer rates at Mach numbers of 4.8 and 6.0. The experimental investigation was conducted on flat plates with sharp leading edges in the Langley 20-inch Mach 6 tunnel and in the Mach number 6.2 blowdown tunnel of the Langley Research Center. The results are compared with the available data, empirical results, and theory from the literature for supersonic and low hypersonic Mach numbers.

SYMBOLS

A_1, A_2	coefficients of T' equation
C_f	local skin-friction coefficient
C_F	average skin-friction coefficient
$c_{p,o}$	specific heat at outer edge of boundary layer
c_w	specific heat of wall material
d	diameter of roughness elements
h	heat-transfer coefficient
k	vertical height of roughness above plate

l length of transition region

M Mach number

N_{Pr} Prandtl number

N_{St} Stanton number

$\dot{q}$ experimental heating rate

r recovery factor

R_k Reynolds number based on fluid conditions at top of roughness elements and height of roughness, $\frac{\rho_k u_k k}{\mu_k}$

R_o unit Reynolds number per foot at outer edge of boundary layer, $\frac{\rho_o u_o}{\mu_o}$

$R_{o,t}$ transition Reynolds number, $\frac{\rho_o u_o t}{\mu_o}$

$R_{o,v}$ local free-stream Reynolds number based on distance from virtual origin, $\frac{\rho_o u_o x_v}{\mu_o}$

$R_{o,x}$ local free-stream Reynolds number based on distance from leading edge, $\frac{\rho_o u_o x}{\mu_o}$

R_{o,x^*} local free-stream Reynolds number based on distance from roughness location, $\frac{\rho_o u_o x^*}{\mu_o}$

$R_{x,T'}$ Reynolds number based on T' conditions and distance from virtual origin, $\frac{\rho' u_o x_v}{\mu'}$

s lateral spacing of roughness

t distance from leading edge to transition (either at end of laminar flow or at beginning of turbulent flow)

T temperature

T' reference temperature

u velocity component of flow parallel to surface of plate

x	distance from leading edge
x_k	distance from leading edge to roughness position
x_v	distance from virtual origin
x^*	distance from roughness to instrumentation location
y	vertical coordinate measured from plate surface
ρ	density
ϕ	leading-edge thickness
θ_w	local wall thickness
τ	time
δ	calculated boundary-layer thickness at roughness position based on velocity
α	angle of attack
γ	ratio of specific heats
μ	viscosity

Subscripts:

1,2,3	denote relative roughness height
cr	critical
k	conditions at top of roughness elements
lam	laminar conditions
o	local conditions at outer edge of boundary layer
r	recovery
T'	based on reference temperature conditions
trans	transitional conditions
turb	turbulent conditions
w	wall

∞ free-stream conditions

Primes denote parameters evaluated at reference temperature T'.

APPARATUS AND TEST METHODS

Wind Tunnel

The test program was conducted in the Langley 20-inch Mach 6 tunnel and in the Mach number 6.2 blowdown tunnel. The Langley 20-inch Mach 6 tunnel is the intermittent type exhausting to the atmosphere through a diffuser augmented by an air ejector. Tests were run with tunnel stagnation pressures of 365, 440, and 515 pounds per square inch absolute with stagnation temperatures of 960° R to 1,020° R. A more detailed description of the tunnel is given in reference 9.

In order to extend the test Reynolds number range below that obtainable in the Langley 20-inch Mach 6 tunnel, additional tests were conducted in the Mach number 6.2 blowdown tunnel. The tunnel is also of the intermittent type exhausting to a 40,000-cubic-foot sphere which can be pumped to pressures as low as 1 millimeter of mercury absolute. Tests were run with tunnel stagnation pressures of approximately 65, 165, and 265 pounds per square inch absolute with stagnation temperatures of 840° to 1,020° R. A more detailed description of the tunnel is given in reference 10.

Models

The models tested consisted of flat plates with sharp leading edges constructed from stainless steel. Each model assembly was 9 inches wide and approximetely 11 inches long for the tests in the Langley 20-inch Mach 6 tunnel. Plate 1 was a continuous plate, a sketch of which is given in figure 1(a). The remaining models consisted of plate 2 with interchangeable leading edges (one for each roughness height). (See fig. 1(b).) The instrumented plates and the leading edges were mounted on a support plate as shown in figure 1. The smaller size of the Mach number 6.2 blowdown tunnel required that the models be smaller. For the tests in this tunnel, plate 2 and the leading edges were cut down so that the model assembly was $7\frac{1}{2}$ inches wide and $10\frac{1}{2}$ inches long.

For the roughness tests, the leading-edge pieces were interchanged, each having a different size roughness mounted 2 inches from the leading edge. Flat plate 2 and the support plate completed the assembly. (See fig. 1(b).) The spheres were glued into small spherical indentations in the leading-edge plate. The location, spacing, height above the plate, and diameter of the spheres are given in figure 1(b).

The leading edge of all the models was a 20° wedge that tapered to a cylindrical leading edge with a radius of approximately 0.002 inch or less. Two models

of each plate were constructed - one being instrumented with 0.050-inch ID pressure orifices and the other with 30-gage iron-constantan thermocouples. The instrumentation was located chordwise along the center line of the plates. The undersurface of each plate instrumented with thermocouples was slotted along the center line to a width of 0.6 inch and a surface skin thickness of approximately 0.020 inch to minimize the lateral heat conduction in the skin.

Test Methods and Techniques

For the tests in the Langley 20-inch Mach 6 tunnel, the free-stream Mach number outside the boundary layer of the models was varied by changing the angle of attack of the plates. This method gave a local surface Mach number M_o of 6.0 at an angle of attack of 0° and of 4.8 at an angle of attack of 8°. The resulting unit Reynolds numbers per foot based on conditions outside the boundary layer were 5.82×10^6, 7.02×10^6, and 8.22×10^6 for $M_o = 6.0$ and 9.84×10^6, 11.86×10^6, and 13.92×10^6 for $M_o = 4.8$ for the tunnel stagnation pressures of 365, 440, and 515 pounds per square inch absolute, respectively.

The tests were run in the Mach number 6.2 blowdown tunnel with the plates at an angle of attack of 0°, a nominal local Mach number of 6.0 being obtained. The resulting local unit Reynolds numbers per foot were approximately 4×10^6, 2.6×10^6, and 1.2×10^6.

Pressure tests.- Pressure distributions along the center line of the plates were obtained in the Langley 20-inch Mach 6 tunnel for $M_o = 6.0$ and 4.8 with free-stream Reynolds numbers per foot of 5.82×10^6, 7.02×10^6, and 8.22×10^6. The local static pressures on the plates were measured by connecting the orifices to pressure-switching devices which in turn connected the orifices in sequence to electrical pressure transducers. The electrical outputs from the transducers were recorded on a digital readout recorder. Each pressure-switching device was connected to two transducers with ranges of 1 and 5 pounds per square inch absolute. The accuracy of the transducers is approximately 1/2 percent of full-scale reading. All pressure tests were run on the same support system as was used for the heat-transfer tests.

Heat-transfer tests.- The aerodynamic heating was determined by the transient calorimetry technique by which the rate of heat storage in the model skin is measured. The models, originally at room temperature or slightly cooler, were suddenly exposed to the air flow by quick injection from a sheltered position beyond the tunnel wall. Injection was accomplished in less than 0.25 second and the model remained in the tunnel for only 4 seconds so that the model was in a nearly isothermal condition, lateral conduction in the skin being kept to a minimum.

Optical methods.- During the pressure and heat-transfer tests in the Langley 20-inch Mach 6 tunnel, shadowgraphs and schlieren photographs were occasionally taken to aid in determining the type of boundary layer existing on the plates.

DATA REDUCTION

The electrical outputs from the thermocouples were recorded on a high-speed digital readout recorder. The reading from each thermocouple was recorded at 0.025-second intervals, converted to a binary digital system, and recorded on magnetic tape. The temperature-time data were fitted to a second-degree curve by the method of least squares, and the time derivative of temperature was computed on a card-programed computer.

The tunnel stagnation temperature range was 840° R to $1,020^{\circ}$ R and the wall temperature of the plate was approximately 550° R. Because of the short time required for the injection of the model, the plates were considered to have been subjected to a step function in the applied heat-transfer coefficient. The thin-skin equation used to calculate the local surface heating rate was

$$\dot{q} = c_w \rho_w \theta_w \frac{dT_w}{d\tau} \tag{1}$$

The measured local heat-transfer coefficient was then calculated by the relation

$$h = \frac{\dot{q}}{T_r - T_w} \tag{2}$$

in which conduction effects are neglected, and where T_r is the calculated recovery temperature defined as

$$T_r = T_o \left[1 + M_o^2 \frac{r(\gamma - 1)}{2} \right]$$

T_w is the measured wall temperature, and M_o is the local Mach number outside the boundary layer calculated from the measured pressure distribution. For the tests in the Mach number 6.2 blowdown tunnel, the pressure distribution was assumed to be the same as that obtained in the Langley 20-inch Mach 6 tunnel for a given configuration. The recovery temperature T_r was calculated by assuming a recovery factor equal to 0.830 in the laminar region and 0.883 in the turbulent region. For the transitional region, T_r was calculated by assuming a linear variation given by

$$T_{r,trans} = T_{r,lam} + \frac{\Delta x}{l}\left(T_{r,turb} - T_{r,lam}\right) \tag{3}$$

where

Δx linear distance from beginning of boundary-layer transition

l length of transition region

Finally, the Stanton number, based on local conditions outside of the boundary layer, was calculated by use of the equation

$$N_{St} = \frac{h}{\rho_o u_o c_{p,o}} \tag{4}$$

The experimental heat-transfer parameters $\dot{q}$, h, and N_{St} presented in this report were determined by reading the slope of the temperature-time curve at a time 0.05 second after the model was in position in the tunnel. The maximum surface temperature increase at the time for which the parameters were calculated was always less than 25° and generally less than 15°. This low temperature increase combined with the thin-skin thickness kept the conduction error at a minimum. The inaccuracy of the distribution is thought to be less than ±10 percent.

REVIEW OF HEAT-TRANSFER EQUATIONS

There are many methods available for the theoretical calculation of the Stanton number. (See, for example, refs. 11 to 16.) In this analysis, the T' method of Monaghan (refs. 13 and 14) has been employed. From reference 16, the T' equation may be written as

$$T' = A_1 T_w + T_o\left[1 - A_1 + A_2\left(\frac{\gamma - 1}{2}\right)M_o^2\right] \tag{5}$$

The Stanton number may be determined from the modified Reynolds analogy

$$N_{St,T'} = \frac{1}{2}\frac{C_{f,T'}}{(N_{Pr})^{2/3}} \tag{6}$$

where the Prandtl number N_{Pr} is based on T' conditions.

Laminar Boundary Layer

For the case of a laminar boundary layer, the coefficients of equation (5) (see ref. 12) become

$$\left.\begin{aligned} A_1 &= 1 - 0.468(N_{Pr})^{1/3} \\ A_2 &= \left(1 - A_1 - 0.273N_{Pr}\right)(N_{Pr})^{1/2} \end{aligned}\right\} \tag{7}$$

By using the Blasius equation for laminar flow, equation (6) becomes

$$N_{St} = \frac{0.332\sqrt{C'}}{\sqrt{R_{o,x}}(N_{Pr})^{2/3}} \tag{8}$$

where N_{St} is based on free-stream conditions for direct comparison with data, and the conversion parameter from T' reference conditions to free-stream conditions C' is given by

$$C' = \frac{\mu'}{\mu_o} \frac{T_o}{T'} \tag{9}$$

Turbulent Boundary Layer

For the case of a turbulent boundary layer, the coefficients of equation (5) (see ref. 13) become

$$\left.\begin{aligned} A_1 &= 0.54 \\ A_2 &= 0.142 \end{aligned}\right\} \tag{10}$$

The Karman-Schoenherr equations were used to determine the local skin-friction coefficient as follows. (See ref. 15 for a plot of these parameters and further discussion.)

$$\frac{0.242}{\sqrt{C_{F,T'}}} = \log_{10}\left(R_{x,T'}\right)\left(C_{F,T'}\right) \tag{11}$$

where

$$R_{x,T'} = \frac{\rho' u_o x_v}{\mu'} \tag{12}$$

$$\frac{C_{f,T'}}{C_{F,T'}} = \frac{1}{1 + 3.59\sqrt{C_{F,T'}}} \tag{13}$$

and $C_{f,T'}$ may be converted to free-stream conditions as follows:

$$C_f = \frac{C_{f,T'}}{T'/T_o} \tag{14}$$

and finally Stanton number is determined by modifying equation (6), basing N_{St} on free-stream conditions so that

$$N_{St} = \frac{1}{2} \frac{C_f}{(N_{Pr})^{2/3}} \tag{15}$$

where C_f is determined by equation (14). The distance x_v of equation (12) is defined as the distance from the virtual origin. In this paper, the virtual origin for the flat plate with undisturbed flow was defined as the point at which laminar flow ends, as determined by the surface heat-transfer rates. (See ref. 15 for further discussion.) For the flat plate with roughness, the virtual origin was found by determining the length of transition l on the smooth plate for a given free-stream Reynolds number, assuming fully developed turbulent flow to begin at the trip position, and then defining the virtual origin to be located at a distance l forward of the trip position.

For the lower Reynolds number tests, fully developed turbulent flow was not obtained on the smooth flat plate; therefore, the length of transition was not known. In order to compare the experimental results with theory for these tests, two theoretical distributions were calculated by:

(1) Assuming the virtual origin to be located at the roughness position $\left(R_{o,v} = R_{o,x*}\right)$

(2) Assuming the Reynolds number based on the virtual origin to be $R_{o,v} = R_{o,x*} + 2.7 \times 10^6$, where 2.7×10^6 was based on the length of transition for the higher Reynolds number tests.

Transitional Boundary Layer

A simple semi-empirical method of predicting the heat transfer in the transitional boundary-layer region has been presented. This method is based on the near linear increase in heat transfer which begins at the end of laminar flow and is presented only for general comparison purposes. In this method, it is assumed that the Stanton number increases linearly from the end of laminar flow to the point at which fully developed turbulent flow is first obtained. The difficulty with the relation is that the beginning and end of transition of the boundary layer must be determined before it can be applied.

RESULTS AND DISCUSSION

Determination of Transition

As has been discussed by Probstein and Lin in reference 2, many factors are known to influence the selection of the so-called "transition point" from laminar to turbulent flow in wind-tunnel tests. For instance, the transition process occurs over a finite distance covering a significant range of Reynolds numbers; and the type of instrumentation and method used to detect transition influences the selection of the transition point.

An accurate method of detecting transition is needed for the proper evaluation of many wind-tunnel test results. In this report, the location of transition has been determined primarily by noting a change in the local surface heating rate along the plates. A typical example of this effect is shown in figure 2 which gives the distribution of the local heating rate along the plate at two local Mach numbers and several unit Reynolds numbers. As the laminar boundary layer on the forward end of the plate thickens, the local heating rate decreases until transition occurs. Once transition of the boundary layer begins, the local heating rate increases rapidly. When fully developed turbulent flow is obtained, the heating rate peaks and begins to decrease with increasing distance from the leading edge. The general shape of the surface-heating-rate distribution is, of course, similar to that of the usual shear distributions for a flat plate. (See, for example, ref. 17.) The locations defined as the beginning and end of the

transition region are sketched on the insert of figure 2(a). The beginning of transition (end of laminar flow) was taken as that region where the heating rate begins to increase rapidly. The end of transition (beginning of fully developed turbulent flow) was taken as that region where the local heating rates begin to level off rapidly. An objection to the surface-heating-rate method of determining transition is the error introduced by lateral thermal conduction in the skin. However, in these tests great care has been taken to minimize the thermal conduction in the skin so that the transition data presented herein are thought to be accurate.

Mach number, Reynolds number, surface roughness, leading-edge thickness, temperature of model, free-stream turbulence, and so forth, all affect the location of transition. Also, the method of detecting transition influences the apparent experimental location of transition. Therefore, as might be expected, a compilation of the available transition data shows considerable scatter. These data were obtained from references 18 to 25 and the present investigation and are presented in figure 3 with transition Reynolds number plotted as a function of Mach number. Reference 25 has indicated that two very important parameters for correlating the data from the various installations are free-stream unit Reynolds number and leading-edge thickness. However, a further correlation of the data in figure 3 is difficult and out of the scope of this paper; rather figure 3 is meant to show that transition data of this investigation agree reasonably well with those found in the literature and that the general trends of the available data indicate that the stability of the boundary layer increases with increasing Mach number above Mach numbers of approximately 3.5 to 4. Similar results have been found by Potter and Whitfield in reference 26 where for a given unit Reynolds number and leading-edge thickness, the transition Reynolds number was found to increase markedly above a free-stream Mach number of approximately 4.0. The transition Reynolds number is shown (in ref. 26) to increase as much as 500 percent in going from a free-stream Mach number of 4.0 to a free-stream Mach number of 8.0.

To complement the data determined by the heat-transfer method, shadowgraph and schlieren photographs (see, for example, refs. 9 and 27) were also employed to detect the location of transition. A typical shadowgraph for the flat plate is shown in figure 4(a). The beginning of a change in the slope of the thick white band represents the beginning of transition. The end of transition is indicated when the band converges to the apparent plate surface. A typical schlieren photograph of the flow over the flat plate is shown in figure 4(b). The beginning of transition is assumed to occur at the point on the schlieren photograph where the boundary layer begins to thicken more rapidly. (See ref. 18.) A comparison of the transition data from the shadowgraph and schlieren photographs with no roughness with that from heat-transfer measurements (fig. 2) as given in figure 3 shows reasonable agreement in the location of transition by the several methods when it is remembered that the beginning of transition is not a point but rather a small region which may shift somewhat with time.

As was pointed out in reference 2, the work of Coles (ref. 20) shows that the Reynolds number for the end of transition differs from the Reynolds number for the beginning of transition by a factor of 1.5 for supersonic Mach numbers. It is interesting to note (from fig. 3) that the data of this investigation fit

approximately this empirical relation for a given free-stream Reynolds number at local free-stream Mach numbers of 4.8 and 6.0.

Effects of Roughness on Boundary-Layer Transition

One of the governing variables in producing transition by three-dimensional roughness elements in supersonic flow is the height of the roughness. Figure 5 presents a sketch typical of the transition positions for various height spheres taken from the data of references 5 and 6 for supersonic flow with zero heat transfer. The different regions of transition as indicated by the curves for various sized roughness are labeled 1, 2, and 3. In zone 1, the free-stream disturbances are predominant in establishing transition, whereas the disturbances from the roughness play the predominant role in zone 3 and a further increase in sphere height has little effect on the location of transition. In zone 2, both the free-stream disturbances and the disturbances created by the roughness have an effect on the position of transition, and a further increase in the height of the roughness will cause the transition location to move forward. The data of reference 5 also indicate that the lateral spacing of a single row of spheres has little effect on boundary-layer transition provided the spheres are not so close together that they act as a two-dimensional roughness element. The effect of sphere spacing was not examined in this test program; however, a roughness element was always located on the center line of the model, forward of the thermocouples (fig. 1) in order to minimize any effect of sphere spacing.

In this paper, a roughness trip is defined as effective (or critical) when a further increase in roughness height causes little change in the forward movement of the location of the end of the boundary-layer transition.

In figures 6 and 7, the distributions of the local heating rates along the plate for various height roughness are presented for local free-stream Mach numbers of 6.0 and 4.8, respectively. In these figures, the data given by the circular symbol represent the heating rates obtained on plate 2 with a sharp leading edge and no roughness. The dashed line represents the faired data from figure 2 for the continuous plate 1. The discrepancy between the two sets of data is thought to result not only from small variations in the leading-edge thickness (see, for example, refs. 25 and 26), but also from a small angle-of-attack variation (less than $1/2^{\circ}$) between the two assemblies. However, the angle of attack for each series of roughness tests was invariant since the data represent a group of tests made without changing the mounting.

Examination of figures 6(a) and 6(c) shows that the smaller diameter roughness elements (k = 0.0018 foot and 0.0030 foot) were actually found to delay transition beyond the transition point found with plate 2 and no roughness. Since these data indicated that small roughness heights may delay transition, further limited roughness tests were conducted with the model assembly having the same leading edge so that possible effects of slight variations in nose bluntness would be eliminated. (This work was stimulated by the comments of Potter and Whitfield in ref. 28 in regard to the summary of this study published in ref. 29.) Figure 6(f) presents the heat flow rate distributions for the model with the same leading edge, and with various height roughness elements at a unit Reynolds number similar to that of figure 6(a). A schematic of the model

shown in the figure illustrates the new mounting technique, the roughness strips being interchangeable and with the same leading edge (thickness diameter of 0.0025 inch), being used for all data of this figure. Comparison of the data in figures 6(a) and 6(f) indicates that although some of the variation in the location of transition with small roughness and no roughness was due to the slight variations in the leading-edge thickness, under certain conditions transition is apparently slightly delayed when the surface roughness is less than the boundary-layer thickness.

The physical reasons for these phenomena are not fully understood; however, reference 19 has indicated that the stability of a separated laminar mixing layer increases with Mach number more rapidly than the stability of an attached laminar boundary layer. This fact has led to the speculation that the laminar separation that must exist near the small roughness elements is at least partially responsible for a delay in the transition at the present Mach number. However, the pressure loss at the edge of the boundary layer caused by the roughness elements may be a contributing factor. These phenomena appear to warrant further investigation.

For the higher Reynolds number tests at $M_o = 6.0$ (figs. 6(a), 6(b), and 6(c)) as the roughness is increased above $k = 0.003$ foot, transition moves forward until a further increase in height is ineffective. For example, note that in figure 6(a) the heating-rate distributions for the roughness of height $k \geqq 0.0054$ foot are approximately the same, and $k = 0.0054$ foot is defined as the roughness height slightly greater than the critical roughness height for this free-stream Reynolds number.

Similar trends are evident in figure 7 for $M_o = 4.8$, the smallest size roughness ($k = 0.0018$ foot) now causing a considerably greater forward movement of the beginning of transition than was found for $M_o = 6.0$, since the local Reynolds number is increased. However, the smallest size roughness is still below the critical height as previously defined.

Previous work has established a criterion for determining the critical height of three-dimensional roughness elements for subsonic and supersonic speeds. (See, for example, refs. 4 and 30.) This criterion states that transition will occur when the roughness Reynolds number exceeds a certain value which is approximately constant with the Mach number. This critical roughness Reynolds number is, by definition, based on the fluid properties at the top of the roughness element and the height of the roughness element. The value of the critical roughness Reynolds number was not found to be affected appreciably by moderate surface cooling. (See ref. 30.)

The variation of roughness Reynolds number R_k with various assumed roughness heights is presented in figures 8 and 9 for local free-stream Mach numbers of 6.0 and 4.8, respectively. These figures show the value of R_k for both adiabatic wall conditions ($T_w/T_r = 1.0$) and the actual wall temperature ($T_w/T_r = 0.66$) of the present tests. The roughness Reynolds numbers presented were determined from boundary-layer temperature and velocity profiles calculated by the Chapman-Rubesin method for an x-distance of 2 inches from the leading edge (the roughness location). A complete discussion of the validity and assumptions of this theory is given in reference 31. The velocity profiles calculated by

this method are also given in figures 8 and 9. In addition, these figures show that the effect of cooling the boundary layer is to cause a thinning of the boundary layer and thereby increase the R_k values for a given height roughness provided the roughness height is less than the boundary-layer thickness.

The critical roughness Reynolds number has been obtained experimentally for lower supersonic Mach numbers by several investigators. A summary of the experimental results from reference 4 (which included data from other sources, including ref. 5) is presented in figure 10 in the form of the variations of $\sqrt{R_{k,cr}}$ with Mach number. Also plotted in this figure are the results of the present investigation where the open symbol indicates that the roughness height is slightly less than the critical height and the solid symbol indicates that the roughness height is slightly greater than the critical height. This figure shows clearly that the critical roughness Reynolds numbers determined experimentally for $M_o = 4.8$ and $M_o = 6.0$ are much larger than those observed in reference 4 for lower supersonic velocities. The critical roughness height of the present tests is also much larger than that predicted by the semi-empirical equation of reference 6, which was determined from experiments conducted at lower supersonic speeds.

It should be mentioned that the definition and determination of the critical Reynolds number for the previous data shown in figure 10 from reference 4 are not exactly the same as that used in the present report. Also, the data of reference 4 were taken under zero heat-transfer conditions. Some possible values based on the end of transition from the data of references 26 and 32 are also shown in figure 10. In reference 32, the end of transition was determined by the shadowgraph method which is similar to the present transition detection method since both methods detect permanent changes in the boundary-layer profiles. The data in figure 10 show that basing the critical Reynolds number on the end of transition gives values which are higher than those given in reference 4.

A modification of the critical roughness correlation parameter R_k has been given by Potter and Whitfield in references 26 and 33. The results of the present investigation agree well with the extrapolated values given in these references where it is predicted that for local hypersonic Mach number and walls at temperatures corresponding to the conditions of the present investigation, the R_k value needed to bring about transition at the roughness elements would be approximately 2.4×10^4. The values of R_k of the present investigation were approximately 2×10^4 to 4×10^4.

The experimental variation of the critical roughness Reynolds number with free-stream unit Reynolds number for a Mach number of 6.0 is shown in figure 11. Included in this figure are both the data taken with one leading edge with roughness elements mounted on an interchangeable strip and the data taken with interchangeable leading edges. The two sets of data do not coincide; however, this condition may be due in part to a different location x_k of the roughness elements. An increase in free-stream unit Reynolds number by a factor of approximately 8 was found to result in an increase in critical roughness Reynolds number by a factor of approximately 4. Hence at a Mach number of 6.0, $R_{k,cr}$ has been found to be sensitive to the free-stream unit Reynolds number.

For local free-stream Mach numbers of 4.8 and 6.0, it has been shown herein that the roughness parameter k/δ must be approximately 2 or greater to move the beginning of fully developed turbulent flow to the region of the roughness. As is pointed out in reference 26, this requirement of a roughness height of twice the boundary-layer thickness may lead to limitations in the use of three-dimensional roughness to obtain turbulent flow in wind-tunnel tests because of the flow distortions created by the roughness extending outside the boundary layer. Of course, the requirement of k/δ values of 2 or greater is partially responsible for the large variation in $R_{k,cr}$ with varying free-stream Reynolds number.

Further work is warranted to give a better insight into the importance of the defining parameters in boundary-layer transition work. It is interesting to note that the recent theoretical investigation of Lees and Reshotho in reference 34 has also indicated that the minimum critical Reynolds number for the boundary layer of an insulated plate would rise sharply with increasing Mach number above a Mach number of 3 and indicates a need for the reexamination of the basic assumption of the theory of stability of the laminar boundary layer at high supersonic and hypersonic Mach numbers.

Comparison of Heat-Transfer Distributions With Theory

Distributions over smooth continuous plate.- The experimental heat-transfer distributions in the form of the variation of Stanton number with distance from the leading edge are shown in figure 12. Also, given in this figure are the calculated variations of Stanton number with distance from the leading edge for the laminar, transitional, and turbulent regions of the boundary layer obtained by the methods presented in the section entitled "Review of Heat-Transfer Equations." This figure clearly shows the relative values of heat transfer to be expected for the various types of local boundary layers with natural transition. The experimental Stanton number is seen to increase by a factor of approximately 3 from the beginning of transition to the end of transition. The calculations predict an increase by a factor of approximately 4; however, the leveling of the experimental heat-transfer values in the rearward portion of the laminar boundary-layer region and the choice of the virtual origin may easily account for the differences between the calculated and experimental values.

Comparison of the theory with the experimental data shows that the theory gives a reasonably good prediction of the magnitude of heat transfer in the laminar region, generally within 15 percent of the experimental value except for the rearward portion of the laminar flow where the experimental heat transfer was found to level off prior to the rapid increase in Stanton number associated with the beginning of transition.

The simple assumption of the virtual origin for the turbulent flow being located at the beginning of transition yields a fair prediction of the heat transfer in the fully developed turbulent boundary-layer region, the maximum deviation between theory and experiment being approximately 30 percent. Note particularly in figure 12(b) that the rate of decrease of turbulent Stanton number with increasing Reynolds number follows very closely the rate of decrease predicted by theory.

The simple empirical relation for the variation of Stanton number in the transition region (given in eq. (15)) also leads to a reasonably good prediction of the experimental results. (Note that the end of transition for the $R_o = 5.82 \times 10^6$ and $M_o = 6.0$ data has been assumed to occur at $x = 11.00$ inches based on the heat-transfer-rate distribution of fig. 2 in the calculation of the Stanton number in the transition region.) Therefore, the difficulty in considering a region in which the boundary layer is transitional is not in determining how the heat transfer associated with the region will vary, but in determining where the laminar flow will end and where the fully developed turbulent flow will begin.

The variation of heat transfer with local Reynolds number for the case of pure laminar flow is shown in figure 13 for the full test range of free-stream unit Reynolds number. The comparison of the experimental data with the theoretical distribution shows that theory gives a good prediction, both of the magnitudes of the data and the slope of the distribution (up to the rearward region of laminar flow where the experimental data are observed to level off prior to transition).

Variation of Stanton number with Reynolds number for turbulent flow.- The variation of the heat transfer with Reynolds number (based on the distance from the virtual origin for the higher Reynolds number tests of the Langley 20-inch Mach 6 tunnel) for the case of fully developed turbulent flow is compared with theory in figure 14. Also in this figure, the experimental turbulent heat-transfer data for the plate with roughness (for values of k equal to or greater than the critical height) are compared with theoretical predictions. The theory is seen to predict reasonably well both the magnitudes and the slopes of data for the plate with and without roughness.

Inspection of figure 14 shows that the highest experimental Stanton number values occur near the roughness position. These peak values of N_{St} decrease slightly as the roughness height is increased above the critical height. Increasing the roughness height apparently has the effect of increasing slightly the effective Reynolds number at any given position. However, the overall reduction in Stanton number with increasing roughness height at any position is rather small since the Stanton number variation is a weak function of Reynolds number for turbulent flow. Therefore, it appears that roughness can be used as a boundary-layer trip for high-speed wind-tunnel tests designed to study heat transfer in a turbulent boundary layer without seriously affecting the heating distribution.

The turbulent Stanton number variation with Reynolds number based on the distance from the roughness location for the complete test range of free-stream unit Reynolds number at a Mach number of 6.0 and roughness of critical height or greater is given in figure 15. As explained previously, for the low Reynolds number tests, fully developed turbulent flow was not obtained so that the length of transition l could not be determined. The assumptions leading to the two theoretical distributions of Stanton number in figure 15 are discussed in the section entitled "Review of Heat-Transfer Equations." Examination of figure 15 shows that the assumption of the virtual origin to be located at the roughness position gives the best agreement with the experimental data over the complete test Reynolds number range.

CONCLUSIONS

An investigation has been conducted in the Langley 20-inch Mach 6 tunnel and in the Mach number 6.2 blowdown tunnel of the Langley Research Center to determine the effects of controlled surface roughness on boundary-layer transition and heat transfer for local free-stream Mach numbers of 6.0 and 4.8. Analysis of the experimental results and comparison with theory and previous results from the literature have led to the following conclusions:

1. A compilation of the current data and the data available from the literature indicates that the Reynolds number required to bring about natural transition increases markedly with increasing Mach number above a Mach number of approximately 3.7.

2. For a Mach number of 6.0, surface roughness that is less than the calculated boundary-layer velocity thickness at the roughness position can under certain conditions delay transition.

3. The critical roughness Reynolds number required to move the beginning of turbulent flow to the region of the roughness is greater for higher supersonic and hypersonic Mach numbers than has been found at lower supersonic speeds.

4. The high values of the required critical roughness Reynolds numbers for the Mach numbers of this investigation led to required roughness heights of approximately twice the calculated boundary-layer thickness at the roughness position. The effect of the large required roughness on the heat-transfer distribution downstream of the roughness has been shown to be small.

5. Theoretical calculations of the heat-transfer distributions agree reasonably well with the experimental data obtained with the smooth flat plate. Also, theoretical calculations of the turbulent heat-transfer data on the plate with roughness of critical height or greater agreed reasonably well when it is assumed that fully developed turbulent flow begins at the roughness position.

Langley Research Center,
National Aeronautics and Space Administration,
Langley Station, Hampton, Va., October 9, 1963.

REFERENCES

1. Low, George M.: Boundary-Layer Transition at Supersonic Speeds. NACA RM E56E10, 1956.

2. Probstein, Ronald F., and Lin, C. C.: A Study of the Transition to Turbulence of the Laminar Boundary Layer at Supersonic Speeds. Preprint No. 596, S.M.F. Fund Preprint, Inst. Aero. Sci., Inc., Jan. 1956.

3. Rubesin, Morris W., Rumsey, Charles B., and Varga, Steven A.: A Summary of Available Knowledge Concerning Skin Friction and Heat Transfer and Its Application to the Design of High-Speed Missiles. NACA RM A51J25a, 1951.

4. Braslow, Albert L.: Review of the Effect of Distributed Surface Roughness on Boundary-Layer Transition. Presented to Meeting of AGARD Wind Tunnel and Model Testing Panel (London, England), Apr. 25-29, 1960.

5. Van Driest, E. R., and McCauley, W. D.: The Effect of Controlled Three-Dimensional Roughness on Boundary-Layer Transition at Supersonic Speeds. Jour. Aero/Space Sci., vol. 27, no. 4, Apr. 1960, pp. 261-271, 303.

6. Van Driest, E. R., and Blumer, C. B.: Boundary-Layer Transition at Supersonic Speeds - Three-Dimensional Roughness Effects (Spheres). Jour. Aerospace Sci., vol. 29, no. 8, Aug. 1962, pp. 909-916.

7. Stetson, Kenneth F.: Boundary-Layer Transition on Blunt Bodies With Highly Cooled Boundary Layers. Jour. Aero/Space Sci., vol. 27, no. 2, Feb. 1960, pp. 81-91.

8. Bertram, M. H., and Wiggs, M. Margarette: Effect of Surface Distortions on the Heat Transfer to a Wing at Hypersonic Speeds. Paper No. 62-127, Inst. Aerospace Sci., June 1962.

9. Sterrett, James R., and Emery, James C.: Extension of Boundary-Layer-Separation Criteria to a Mach Number of 6.5 by Utilizing Flat Plates With Forward-Facing Steps. NASA TN D-618, 1960.

10. Jones, Robert A., and Gallagher, James J.: Heat-Transfer and Pressure Distributions of a 60° Swept Delta Wing With Dihedral at a Mach Number of 6 and Angles of Attack From 0° to 52°. NASA TM X-544, 1961.

11. Seiff, Alvin: Examination of the Existing Data on the Heat Transfer of Turbulent Boundary Layers at Supersonic Speeds From the Point of View of Reynolds Analogy. NACA TN 3284, 1954.

12. Monaghan, R. J.: An Approximate Solution of the Compressible Laminar Boundary Layer on a Flat Plate. R. & M. No. 2760, British A.R.C., 1956.

13. Monaghan, R. J.: On the Behavior of Boundary Layers at Supersonic Speeds. Fifth International Aeronautical Conference (Los Angeles, Calif., June 20-23, 1955), Inst. Aero. Sci., Inc., 1955, pp. 277-315.

14. Rubesin, M. W., and Johnson, H. A.: A Critical Review of Skin-Friction and Heat-Transfer Solutions of the Laminary Boundary Layer of a Flat Plate. Trans. A.S.M.E., vol. 71, no. 4, May 1949, pp. 383-388.

15. Peterson, John B., Jr.: A Comparison of Experimental and Theoretical Results for the Compressible Turbulent-Boundary-Layer Skin Friction With Zero Pressure Gradient. NASA TN D-1795, 1963.

16. Bertram, Mitchel H.: Calculations of Compressible Average Turbulent Skin Friction. NASA TR R-123, 1962.

17. Matting, Fred W., Chapman, Dean R., Nyholm, Jack R., and Thomas, Andrew G.: Turbulent Skin Friction at High Mach Numbers and Reynolds Numbers in Air and Helium. NASA TR R-82, 1961.

18. O'Donnell, Robert M.: Experimental Investigation at a Mach Number of 2.41 of Average Skin-Friction Coefficients and Velocity Profiles for Laminar and Turbulent Boundary Layers and an Assessment of Probe Effects. NACA TN 3122, 1954.

19. Chapman, Dean R., Kuehn, Donald M., and Larson, Howard K.: Investigation of Separated Flows in Supersonic and Subsonic Streams With Emphasis on the Effect of Transition. NACA Rep. 1356, 1958. (Supersedes NACA TN 3869.)

20. Coles, Donald: Measurements of Turbulent Friction on a Smooth Flat Plate in Supersonic Flow. Jour. Aero. Sci., vol. 21, no. 7, July 1954, pp. 433-448.

21. Brinich, Paul F., and Diaconis, Nick S.: Boundary-Layer Development and Skin Friction at Mach Number 3.05. NACA TN 2742, 1952.

22. Brinich, Paul F.: Boundary-Layer Transition at Mach 3.12 With and Without Single Roughness Elements. NACA TN 3267, 1954.

23. Landis, Fred, Fink, Martin R., and Rosenberg, Murray H.: Boundary-Layer Transition Measurements at Mach Numbers From 5.4 to 7.4. Jour. Aerospace Sci. (Readers' Forum), vol. 27, no. 9, Sept. 1960, pp. 719-720.

24. Korkegi, Robert H.: Transition Studies and Skin-Friction Measurements on an Insulated Flat Plate at a Mach Number of 5.8. Jour. Aero. Sci., vol. 23, no. 2, Feb. 1956, pp. 97-107, 192.

25. Bertram, Mitchel H.: Exploratory Investigation of Boundary-Layer Transition on a Hollow Cylinder at a Mach Number of 6.9. NACA Rep. 1313, 1957. (Supersedes NACA TN 3546.)

26. Potter, J. Leith, and Whitfield, Jack D.: Effects of Unit Reynolds Number, Nose Bluntness, and Roughness on Boundary Layer Transition. AEDC-TR-60-5 (Contract No. AF 40(600)-800), Arnold Eng. Dev. Center, Mar. 1960.

27. Pearcey, H. H.: The Indication of Boundary-Layer Transition on Aerofoils in the N.P.L. 20 in. × 8 in. High Speed Wind Tunnel. C.P. No. 10, British A.R.C., 1950.

28. Potter, J. Leith, and Whitfield, Jack D.: Comment on "Effects of Controlled Roughness on Boundary-Layer Transition at a Mach Number of 6.0." AIAA Jour. (Tech. Comments), vol. 2, no. 2, Feb. 1964, pp. 407-408.

29. Sterrett, James R., and Holloway, Paul F.: Effects of Controlled Roughness on Boundary-Layer Transition at a Mach Number of 6.0. AIAA Jour. (Tech. Notes and Comments), vol. 1, no. 8, Aug. 1963, pp. 1951-1953.

30. Braslow, Albert L.: Effect of Distributed Granular-Type Roughness on Boundary-Layer Transition at Supersonic Speeds With and Without Surface Cooling. NACA RM L58A17, 1958.

31. Chapman, Dean R., and Rubesin, Morris W.: Temperature and Velocity Profiles in the Compressible Laminar Boundary Layer With Arbitrary Distribution of Surface Temperature. Jour. Aero. Sci., vol. 16, no. 9, Sept. 1949, pp. 547-565.

32. Jones, Robert A.: An Experimental Study at a Mach Number of 3 of the Effect of Turbulence Level and Sandpaper-Type Roughness on Transition on a Flat Plate. NASA MEMO 2-9-59L, 1959.

33. Potter, J. Leith, and Whitfield, Jack D.: The Relation Between Wall Temperature and the Effect of Roughness on Boundary-Layer Transition. Jour. Aerospace Sci. (Readers' Forum), vol. 28, no. 8, Aug. 1961, pp. 663-664.

34. Lees, Lester, and Reshotko, Eli: Stability of the Compressible Laminar Boundary Layer. Jour. Fluid Mech., vol. 12, pt. 4, 1962, pp. 555-590.

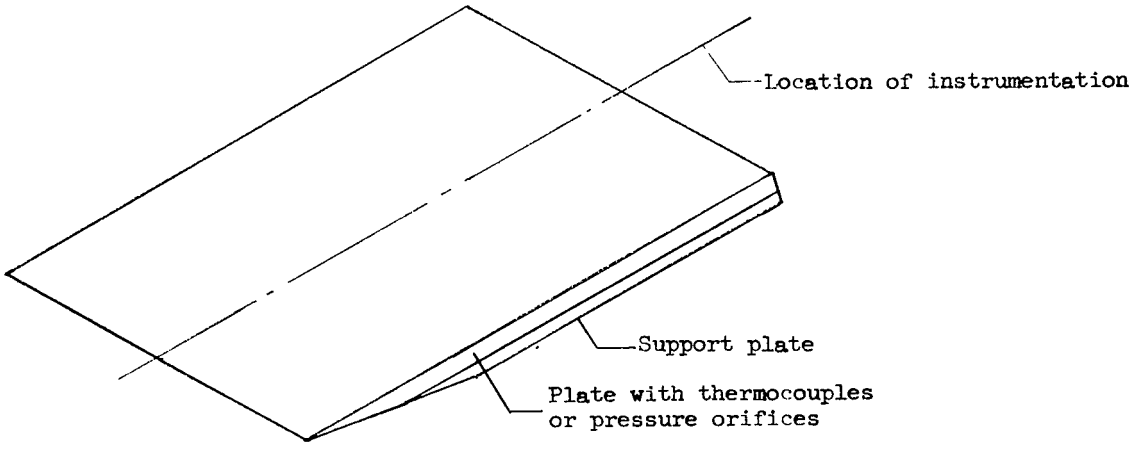

(a) Continuous flat plate 1.

Characteristics of spheres

k	d	s	x_k
0	0	0	
.0018	.0026	.0167	.167
.0030	.0039	.0167	.167
.0044	.0053	.0167	.167
.0054	.0065	.0260	.167
.0067	.0078	.0260	.167
.0091	.0104	.0260	.167

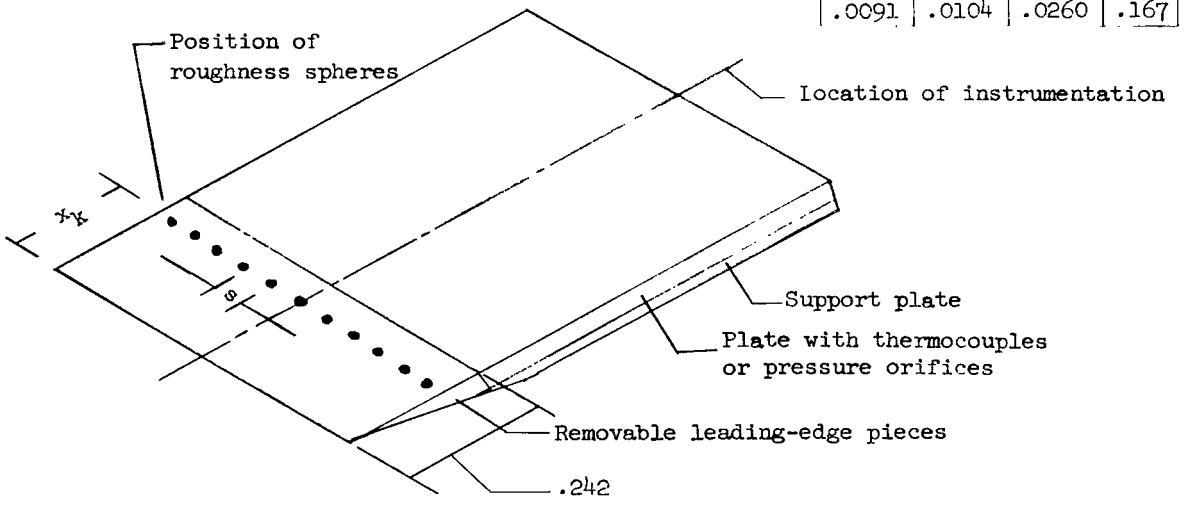

(b) Flat plate 2 with roughness elements.

Figure 1.- Sketch of model assembly. All dimensions are in feet.

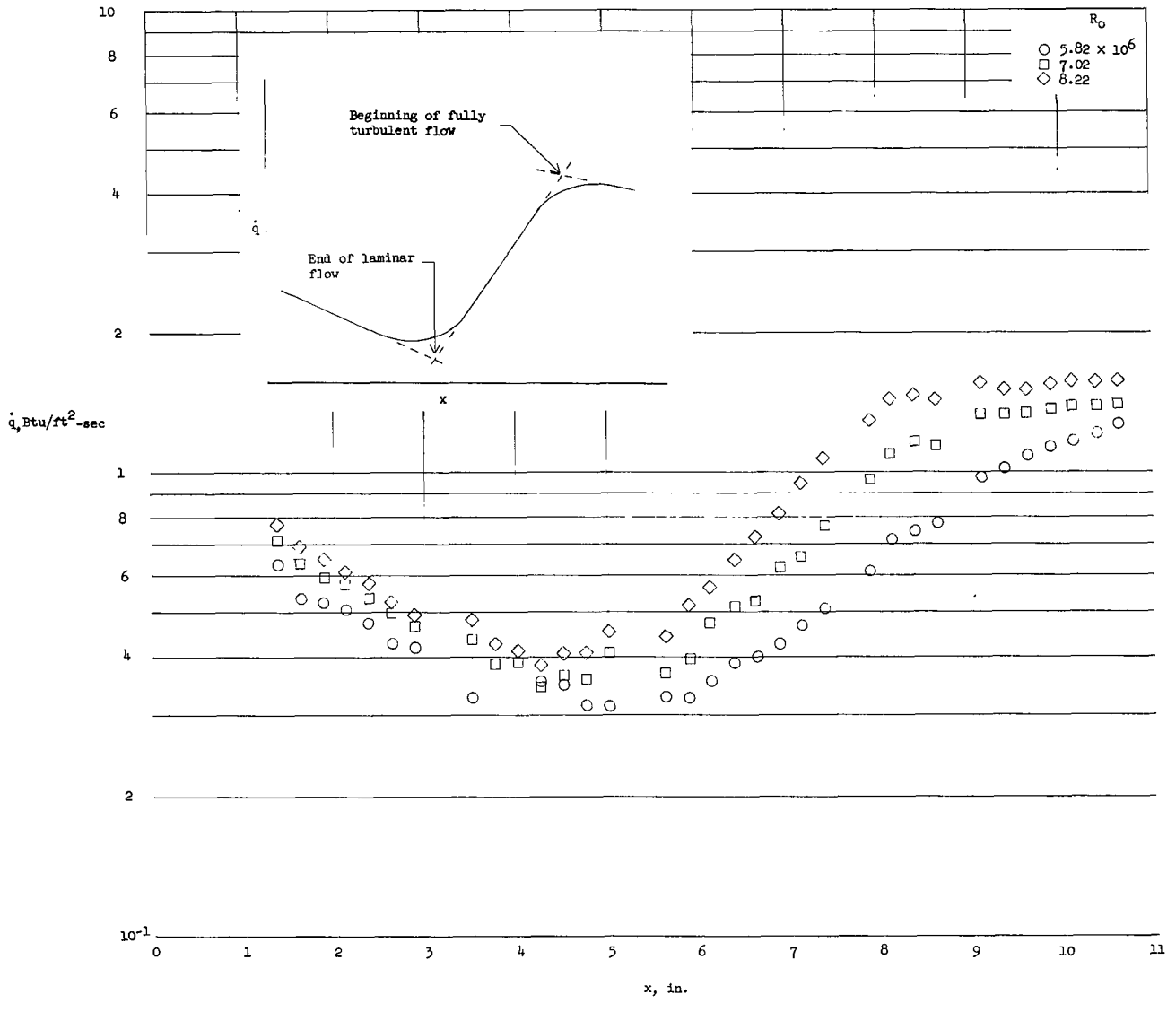

(a) $M_o = 6.0$.

Figure 2.- Heating-rate distribution on the continuous flat plate.

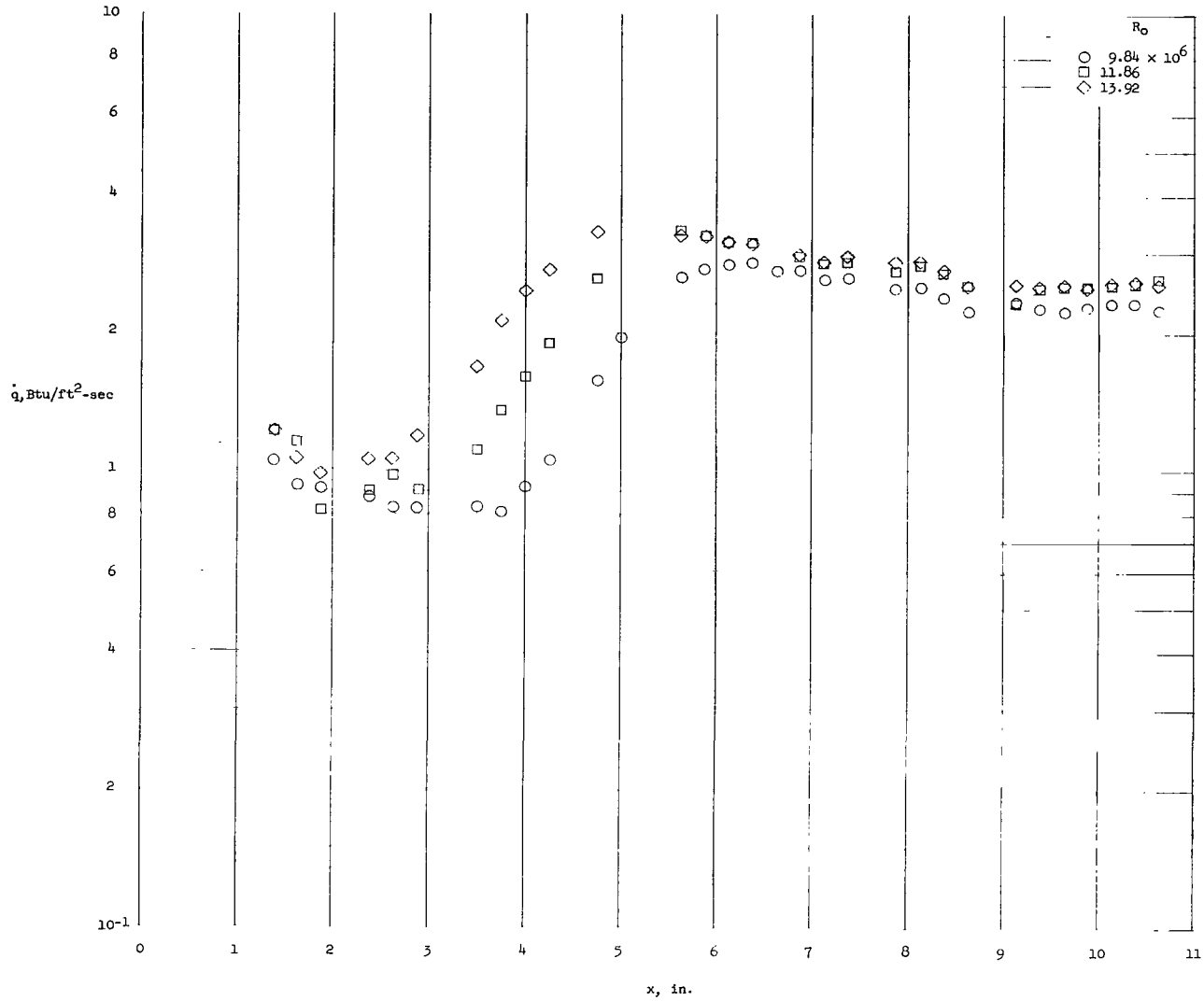

(b) $M_o = 4.80$.

Figure 2.- Concluded.

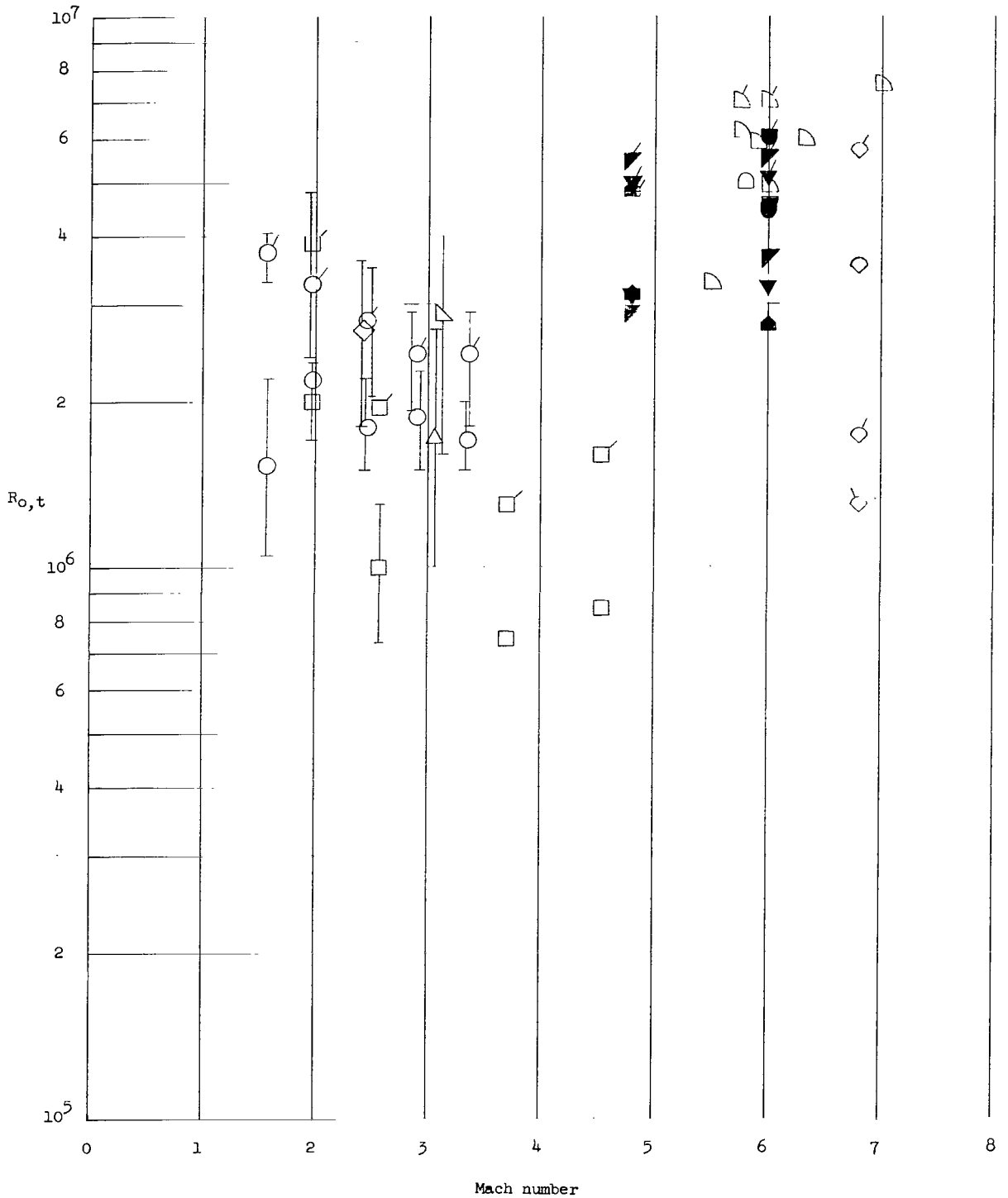

Figure 3.- Variation of transition Reynolds number with Mach number.

Symbol	M	ϕ, in.	R_o/in.	Model	Method	Reference
					Shadowgraph -	
○	1.57	0.005	2.2 × 10^5 to 6.9 × 10^5	Flat plate	transition begins	Chapman, et al.; ref. 19
○	1.57	.005	4.7 to 8.1	Flat plate	transition ends	Chapman, et al.; ref. 19
○	1.96	.005	2.6 to 9.7	Flat plate	transition begins	Chapman, et al.; ref. 19
○	1.96	.005	3.5 to 9.7	Flat plate	transition ends	Chapman, et al.; ref. 19
○	2.44	.005	2.6 to 7.5	Flat plate	transition begins	Chapman, et al.; ref. 19
○	2.44	.005	3.1 to 7.5	Flat plate	transition ends	Chapman, et al.; ref. 19
○	2.90	.005	2.3 to 6.8	Flat plate	transition begins	Chapman, et al.; ref. 19
○	2.90	.005	2.8 to 6.8	Flat plate	transition ends	Chapman, et al.; ref. 19
○	3.34	.005	2.4 to 5.5	Flat plate	transition begins	Chapman, et al.; ref. 19
○	3.34	.005	3.0 to 5.5	Flat plate	transition ends	Chapman, et al.; ref. 19
□	1.97	.001	1.5	Flat plate	Minimum shearing stress	Coles; ref. 20
□	1.97	.001	3.0	Flat plate	Maximum shearing stress	Coles; ref. 20
□	2.57	.001	.59 to 2.5	Flat plate	Minimum shearing stress	Coles; ref. 20
□	2.57	.001	1.6	Flat plate	Maximum shearing stress	Coles; ref. 20
□	3.70	.001	1.4	Flat plate	Minimum shearing stress	Coles; ref. 20
□	3.70	.001	1.0	Flat plate	Maximum shearing stress	Coles; ref. 20
□	4.54	.001	1.6	Flat plate	Minimum shearing stress	Coles; ref. 20
□	4.54	.001	1.2	Flat plate	Maximum shearing stress	Coles; ref. 20
◇	2.41	.002	2.5 to 9.3	Hollow cylinder	Schlieren	O'Donnel; ref. 18
△	3.05	.002 to 0.006	.92 to 5.75	Hollow cylinder	Schlieren	Brinich and Diaconis; ref. 21
▷	3.12	.003	1.0 to 6.5	Flat plate	Surface temperature	Brinich; ref. 22
▷	5.50	.009	2.0	Flat plate	Surface temperature	Landis, et al.; ref. 23
▷	5.75	.009	5.0	Flat plate	Surface temperature	Landis, et al.; ref. 23
▷	5.75	.009	6.0	Flat plate	Surface temperature	Landis, et al.; ref. 23
▷	5.90	.009	5.0	Flat plate	Surface temperature	Landis, et al.; ref. 23
▷	6.00	.009	4.0	Flat plate	Surface temperature	Landis, et al.; ref. 23
▷	6.00	.009	5.0	Flat plate	Surface temperature	Landis, et al.; ref. 23
▷	6.35	.009	4.0	Flat plate	Surface temperature	Landis, et al.; ref. 23
▷	7.00	.009	4.0	Flat plate	Surface temperature	Landis, et al.; ref. 23
▷	5.80	----------	3.0	Flat plate	Luminescent lacquer	Korkegi; ref. 24
◇	6.80	.003 to .005	2.5, 4.0	Hollow cylinder	Shadowgraph	Bertram; ref. 25
◇	6.80	.001 to .003	2.5	Hollow cylinder	Schlieren	Bertram; ref. 25
◇	6.80	.003 to .005	1.4	Hollow cylinder	Shadowgraph	Bertram; ref. 25
◇	6.80	.002	1.55 to 1.75	Hollow cylinder	Shadowgraph, schlieren	Bertram; ref. 25
◆	4.80	.002	8.19	Flat plate	Heat flow rate, end of laminar flow	Current investigation
◆	4.80	.002	9.88	Flat plate	Heat flow rate, end of laminar flow	Current investigation
◆	4.80	.002	11.6	Flat plate	Heat flow rate, end of laminar flow	Current investigation
◆	4.80	.002	8.19	Flat plate	Heat flow rate, beginning of fully turbulent flow	Current investigation
◆	4.80	.002	9.88	Flat plate	Heat flow rate, beginning of fully turbulent flow	Current investigation
◆	4.80	.002	11.6	Flat plate	Heat flow rate, beginning of fully turbulent flow	Current investigation
◆	6.00	.002	4.85	Flat plate	Heat flow rate, end of laminar flow	Current investigation
◆	6.00	.002	5.85	Flat plate	Heat flow rate, end of laminar flow	Current investigation
◆	6.00	.002	6.85	Flat plate	Heat flow rate, end of laminar flow	Current investigation
◆	6.00	.002	5.85	Flat plate	Heat flow rate, beginning of fully turbulent flow	Current investigation
◆	6.00	.002	6.85	Flat plate	Heat flow rate, beginning of fully turbulent flow	Current investigation
◆	6.00	.002	6.85	Flat plate	Schlieren	Current investigation
◆	6.00	.002	6.85	Flat plate	Shadowgraph, end of laminar flow	Current investigation
◆	6.00	.002	6.85	Flat plate	Shadowgraph, beginning of fully turbulent flow	Current investigation

Figure 3.- Concluded.

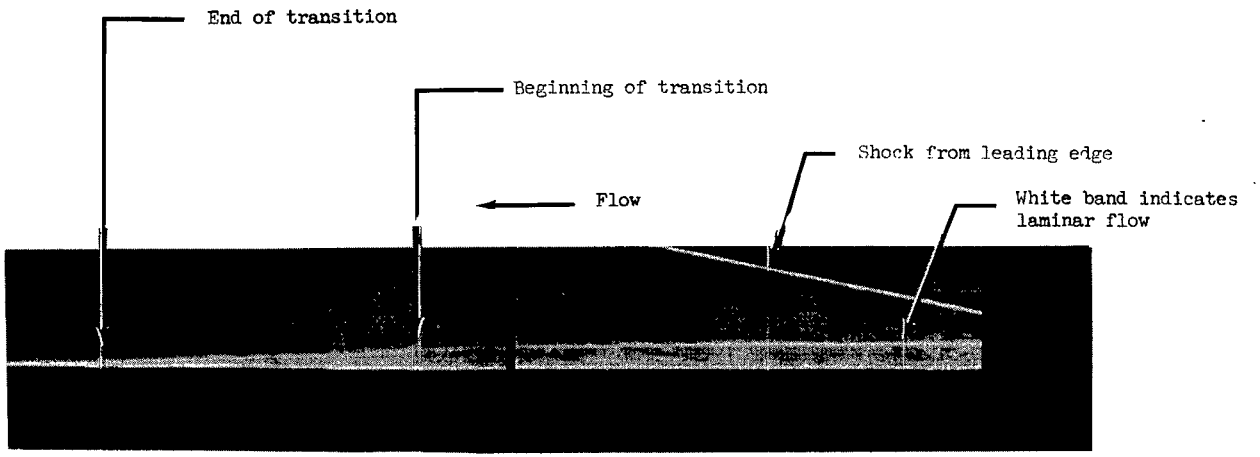

(a) Shadowgraph.

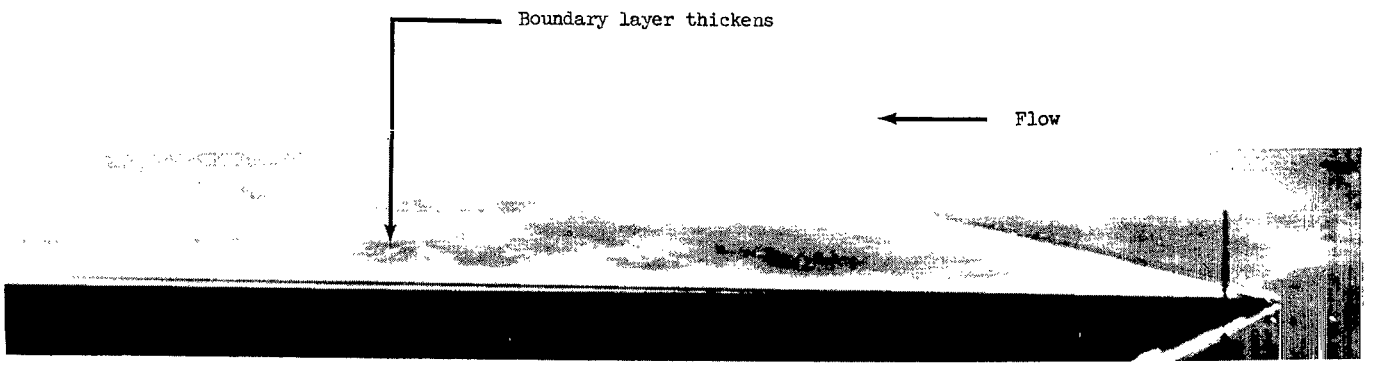

(b) Schlieren photograph.

Figure 4.- Shadowgraph and schlieren photograph of flow over the flat plate. $M_o = 6.0$; $R_o = 8.22 \times 10^6$.

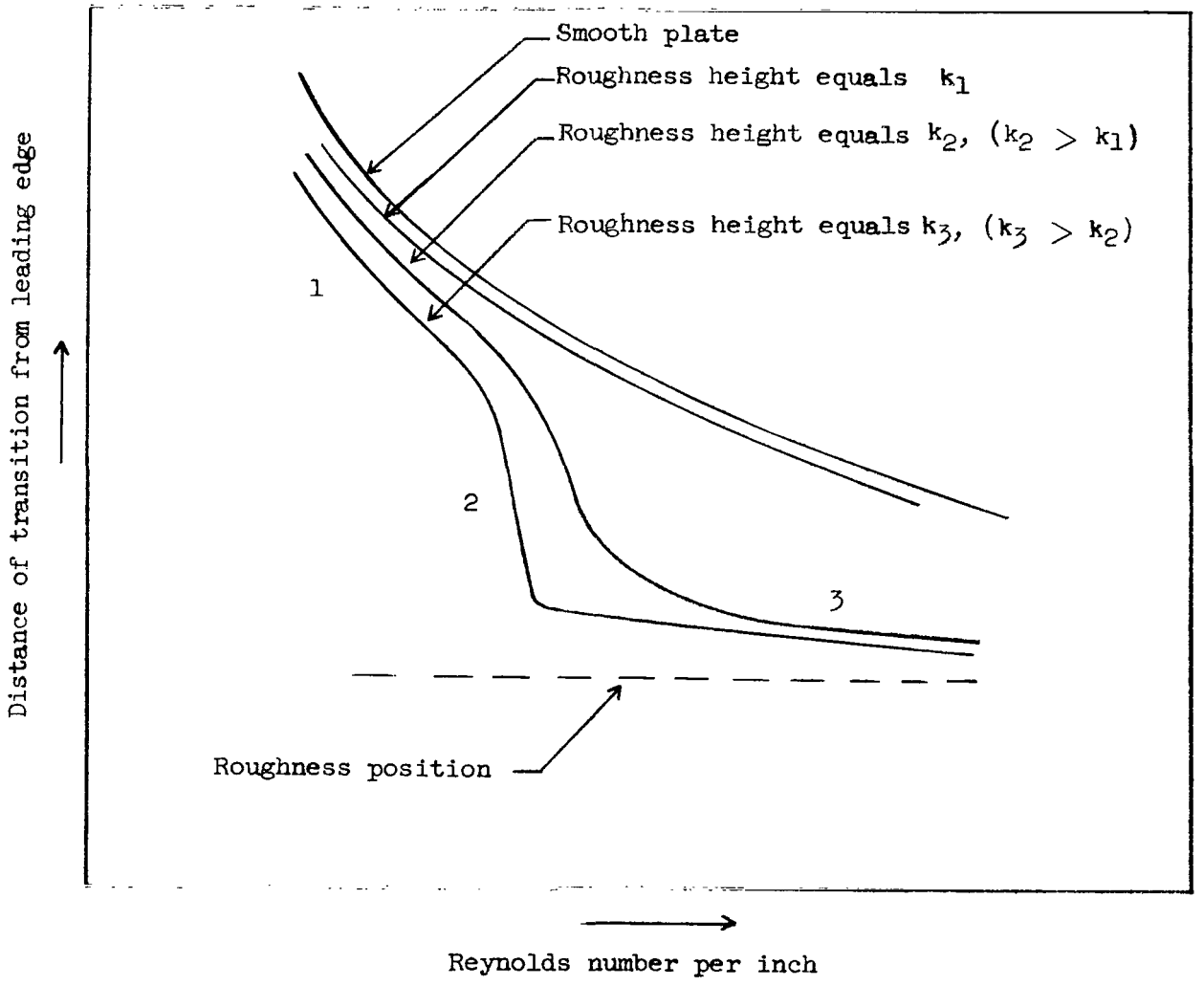

Figure 5.- Sketch showing variation of transition location with Reynolds number for various size surface roughness elements.

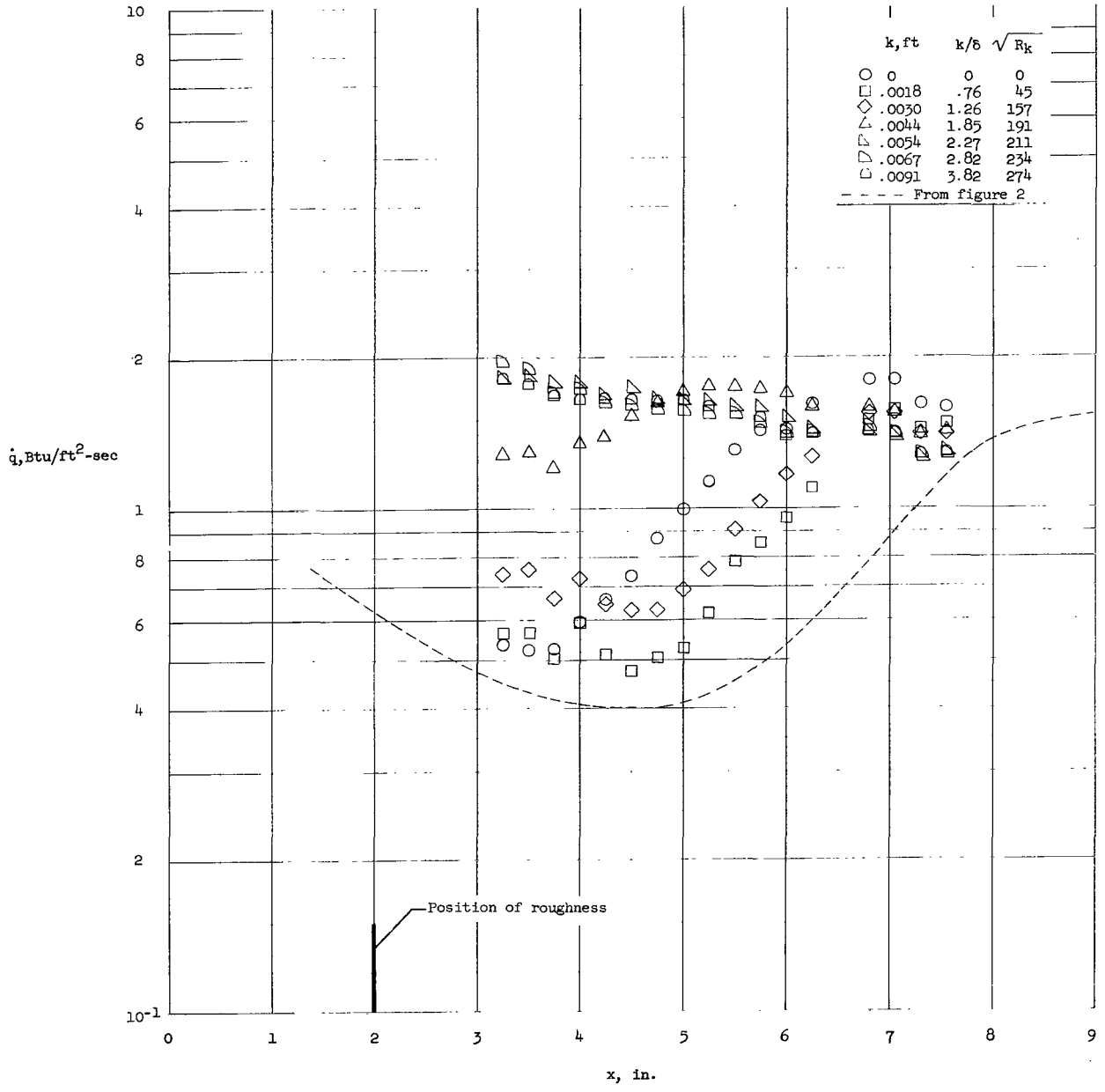

(a) Interchangeable leading edges; $R_o \approx 8.2 \times 10^6$.

Figure 6.- Heating-rate distribution on plate 2 for various size spheres. $M_o = 6.0$.

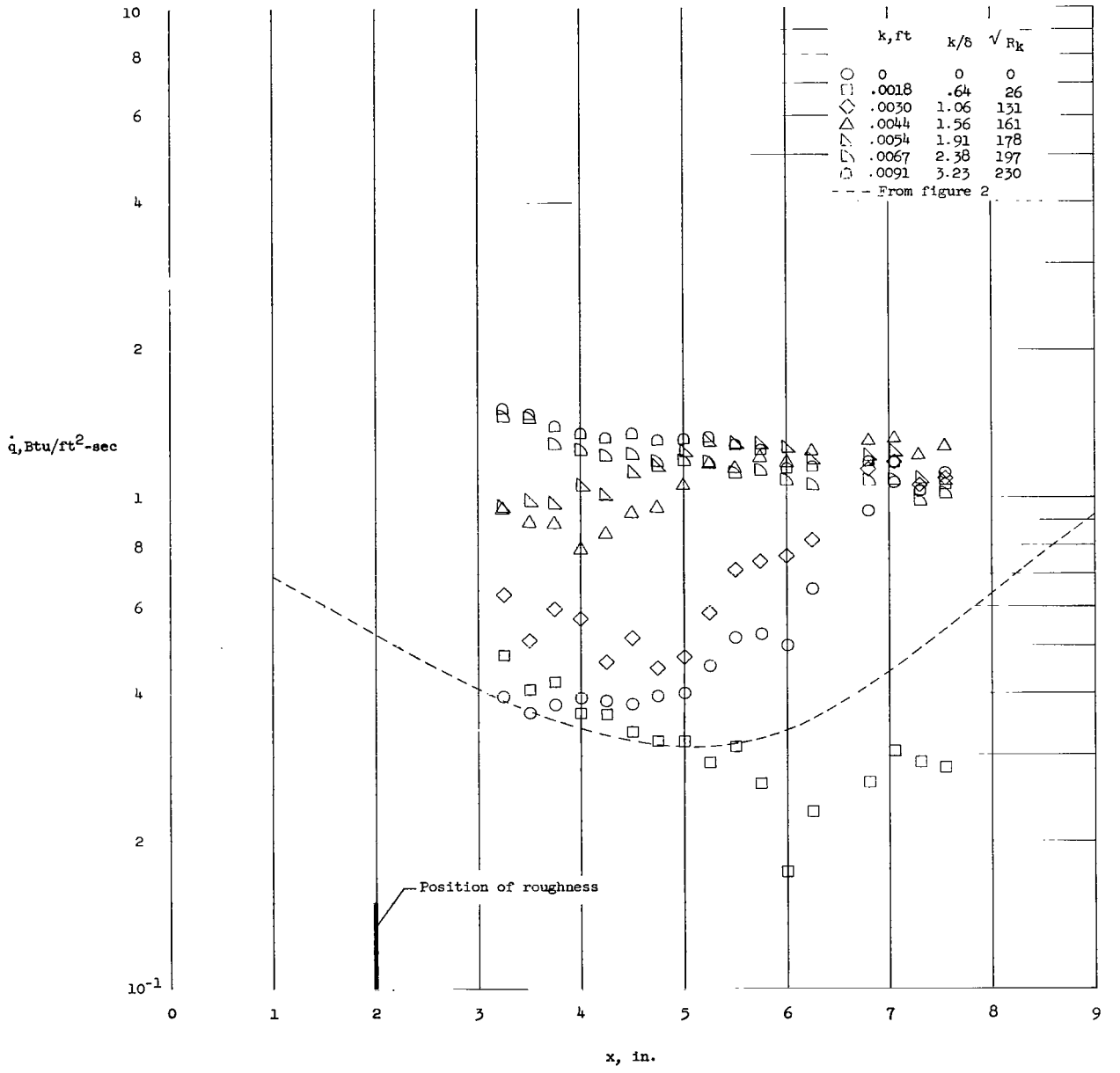

(b) Interchangeable leading edges; $R_o \approx 5.8 \times 10^6$.

Figure 6.- Continued.

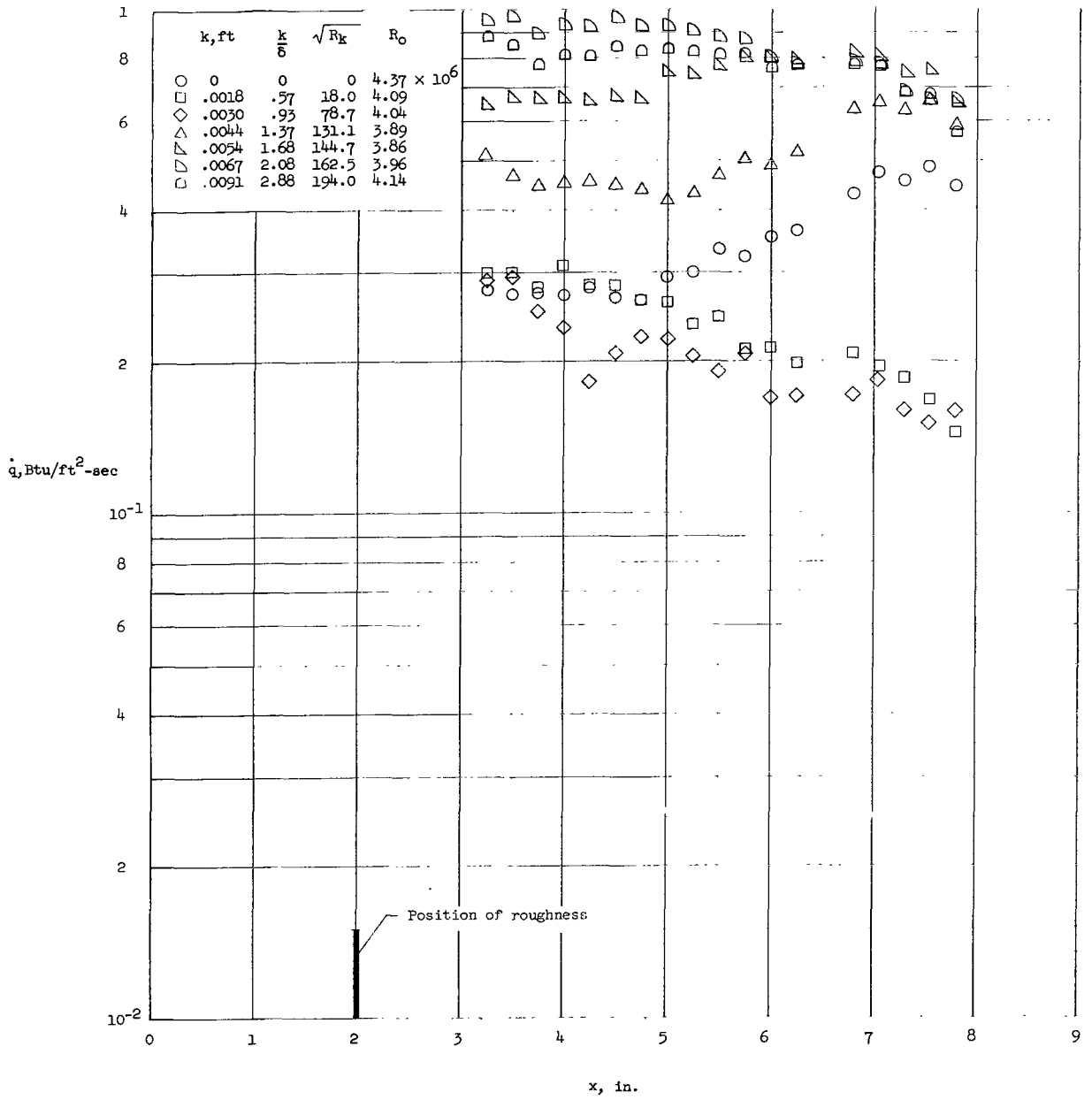

(c) Interchangeable leading edges; $R_o \approx 4 \times 10^6$.

Figure 6.- Continued.

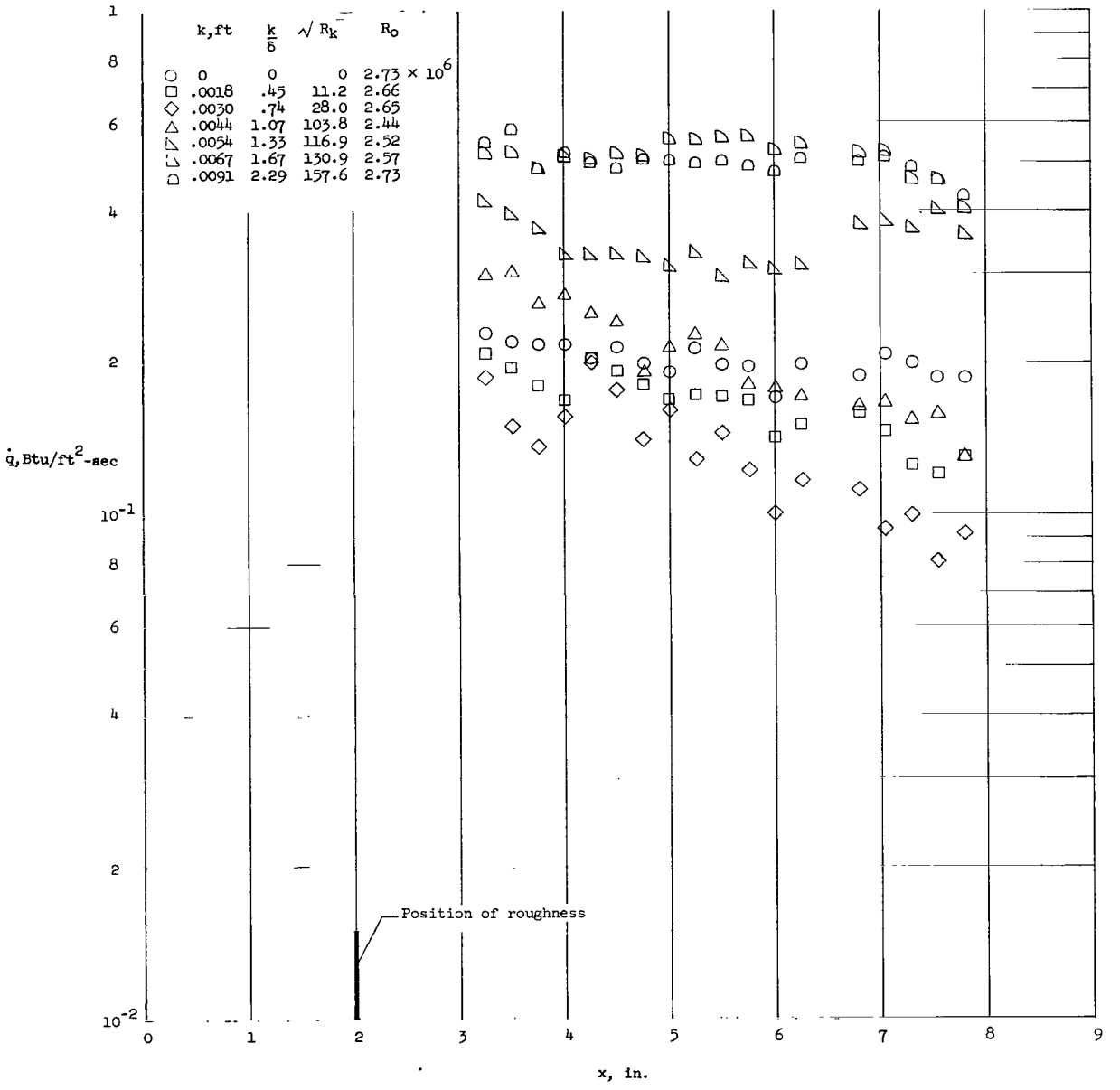

(d) Interchangeable leading edges; $R_o \approx 2.6 \times 10^6$.

Figure 6.- Continued.

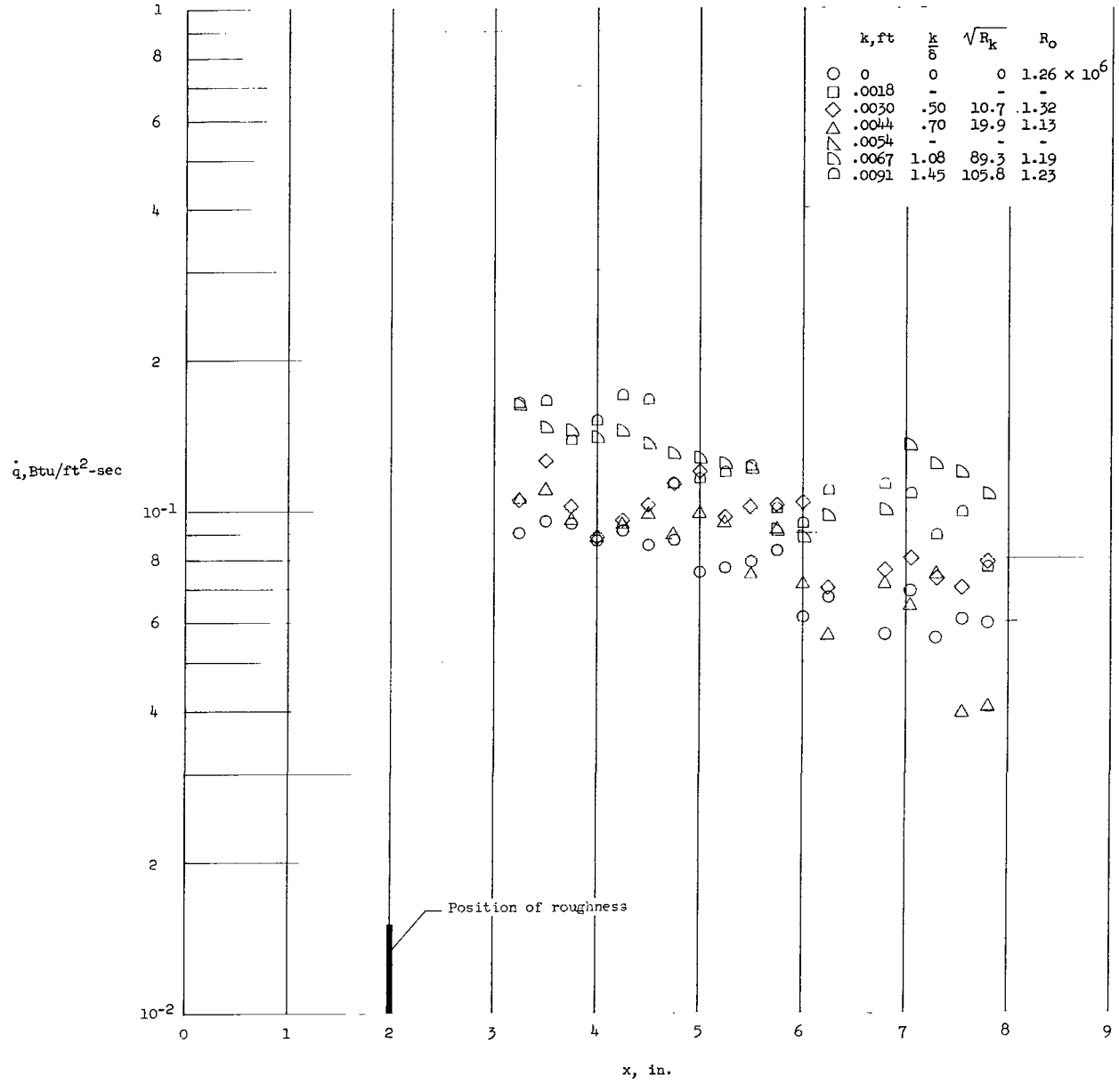

(e) Interchangeable leading edges; $R_o \approx 1.2 \times 10^6$.

Figure 6.- Continued.

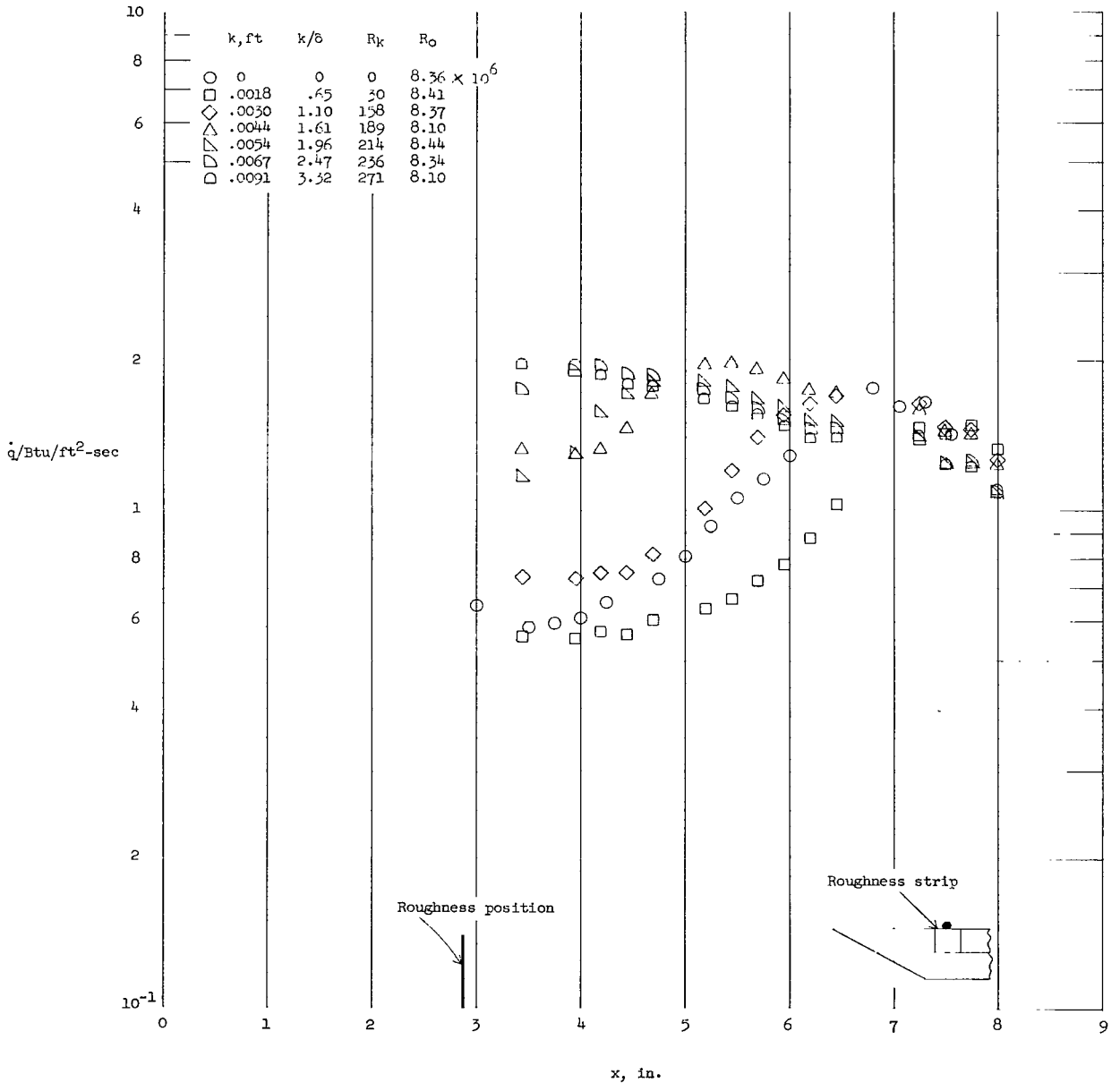

(f) One leading edge, interchangeable roughness strip, $R_o \approx 8.2 \times 10^6$.

Figure 6.- Concluded.

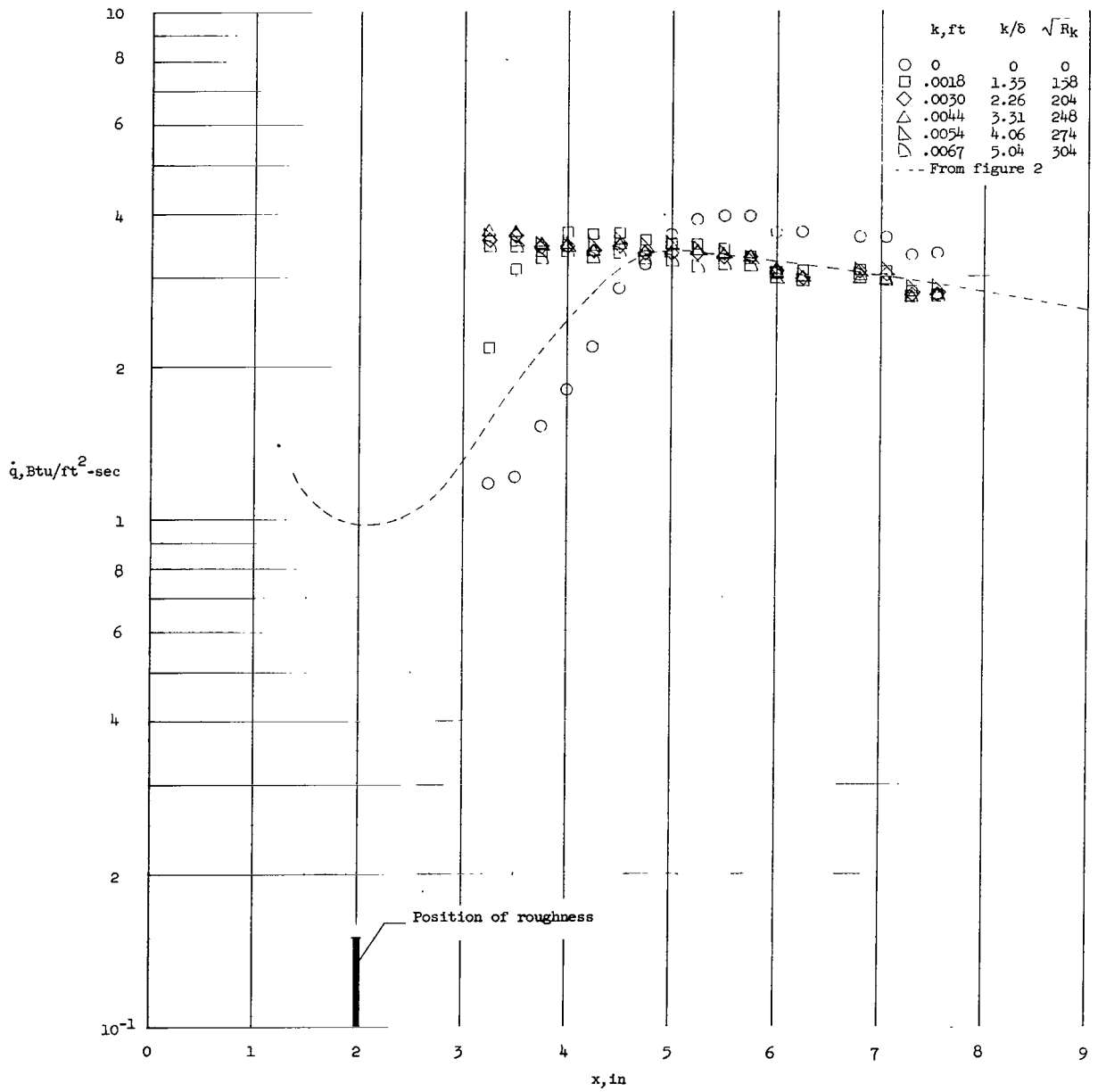

(a) Interchangeable leading edges; $R_o \approx 13.9 \times 10^6$.

Figure 7.- Heating-rate distributions on plate 2 for various size spheres. $M_o = 4.8$.

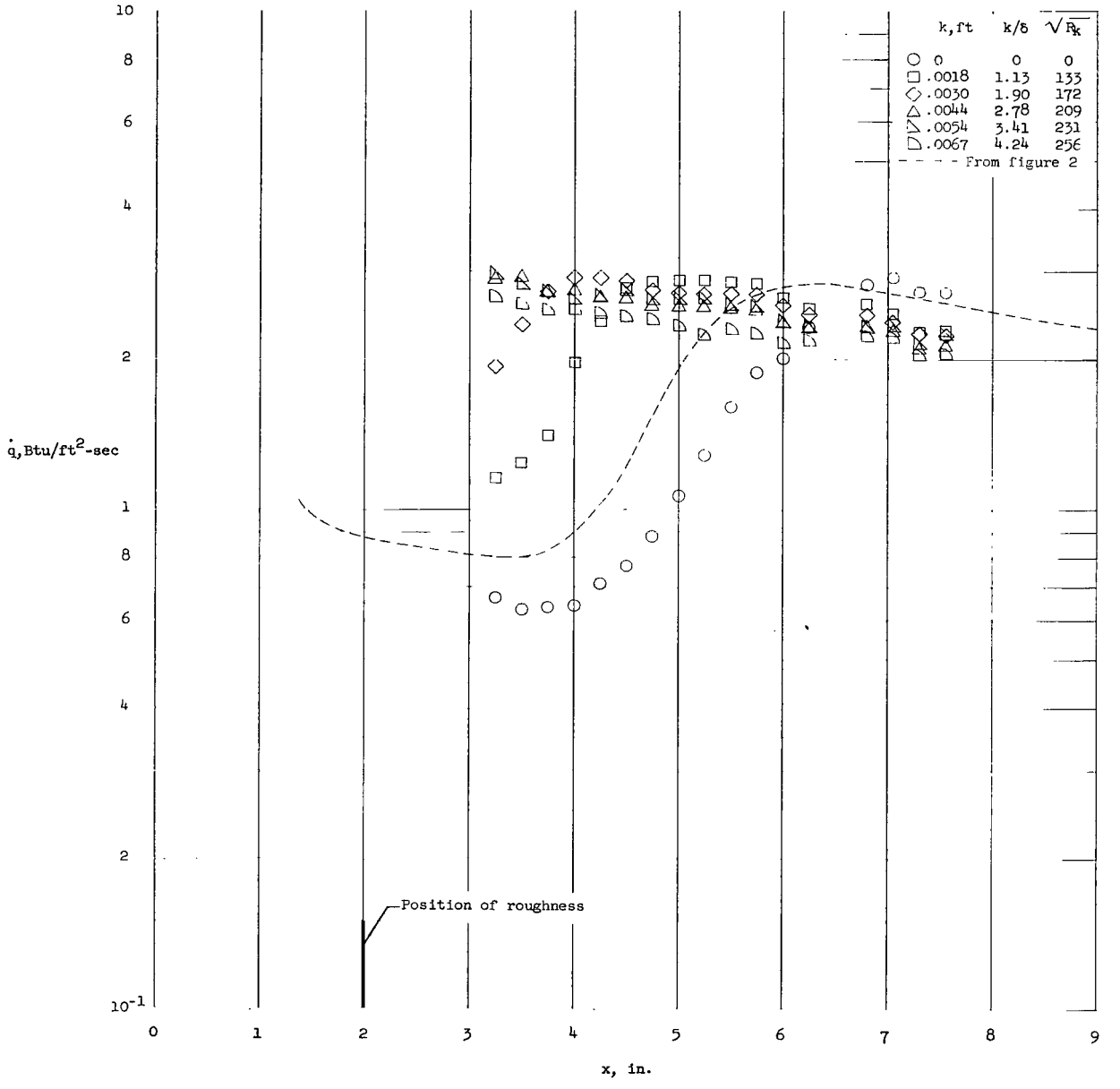

(b) Interchangeable leading edges; $R_o \approx 9.8 \times 10^6$.

Figure 7.- Concluded.

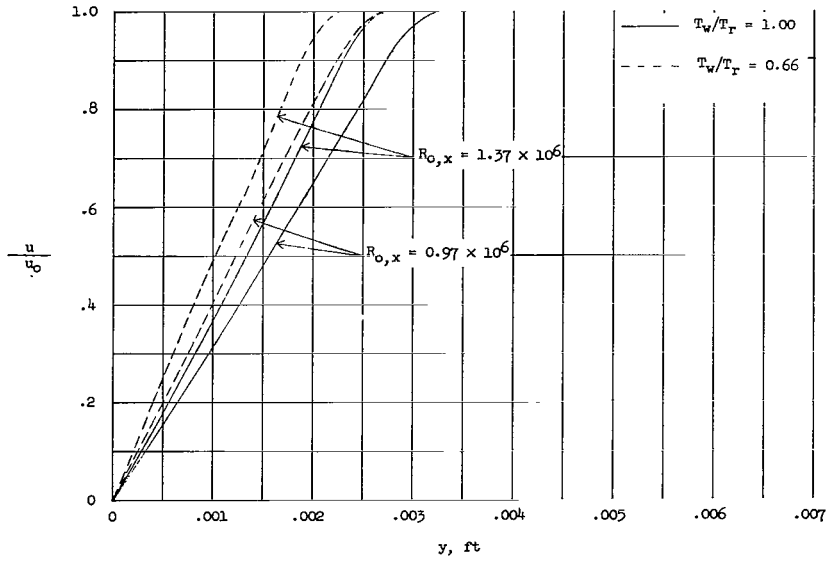

(a) Velocity profiles.

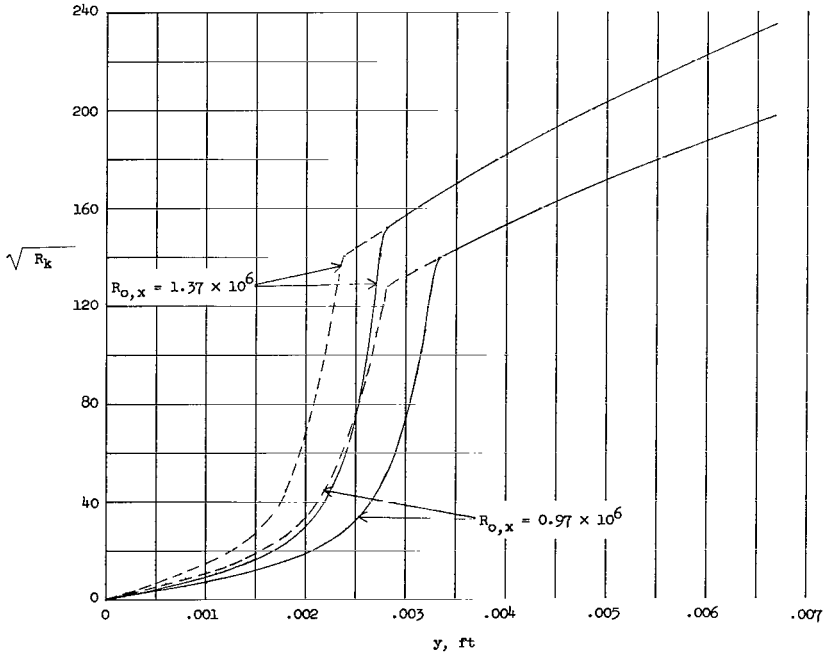

(b) R_k values.

Figure 8.- Calculated boundary-layer velocity profiles and corresponding R_k values for M_o = 6.0. x = 0.167 feet.

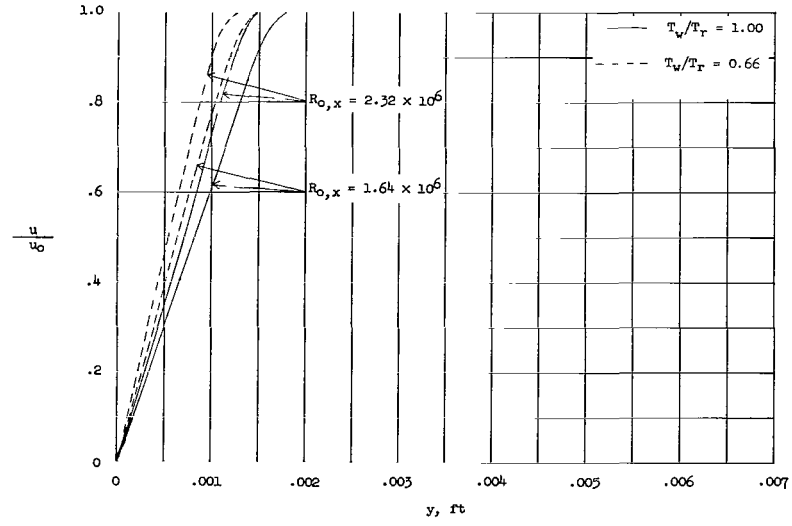

(a) Velocity profiles.

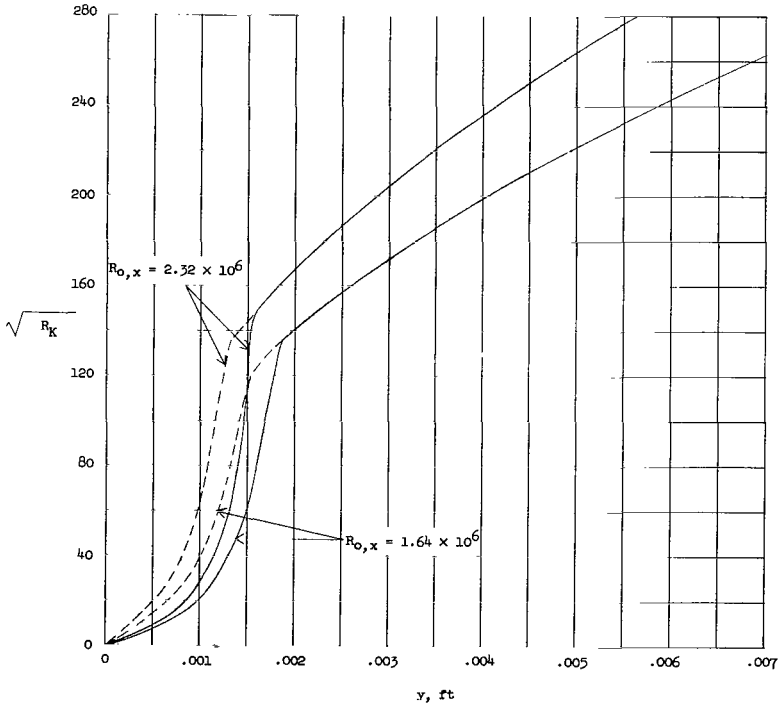

(b) R_K values.

Figure 9.- Calculated boundary-layer velocity profiles and corresponding R_K values for M_o = 4.8. x = 0.167 feet.

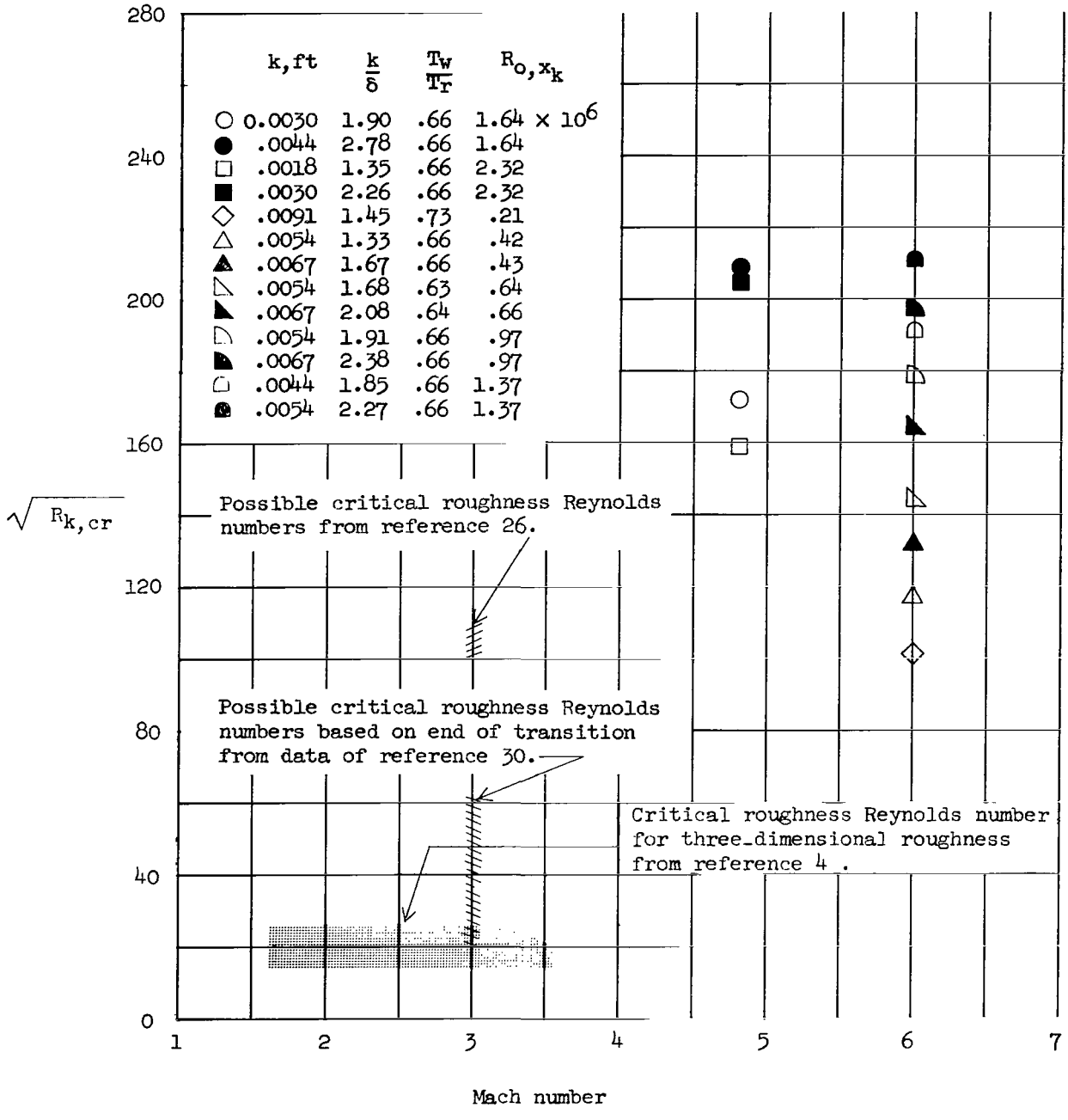

Figure 10.- Critical roughness Reynolds number at several Mach numbers. Open symbols indicate k slightly less than the critical value and solid symbols indicate k slightly greater than the critical value.

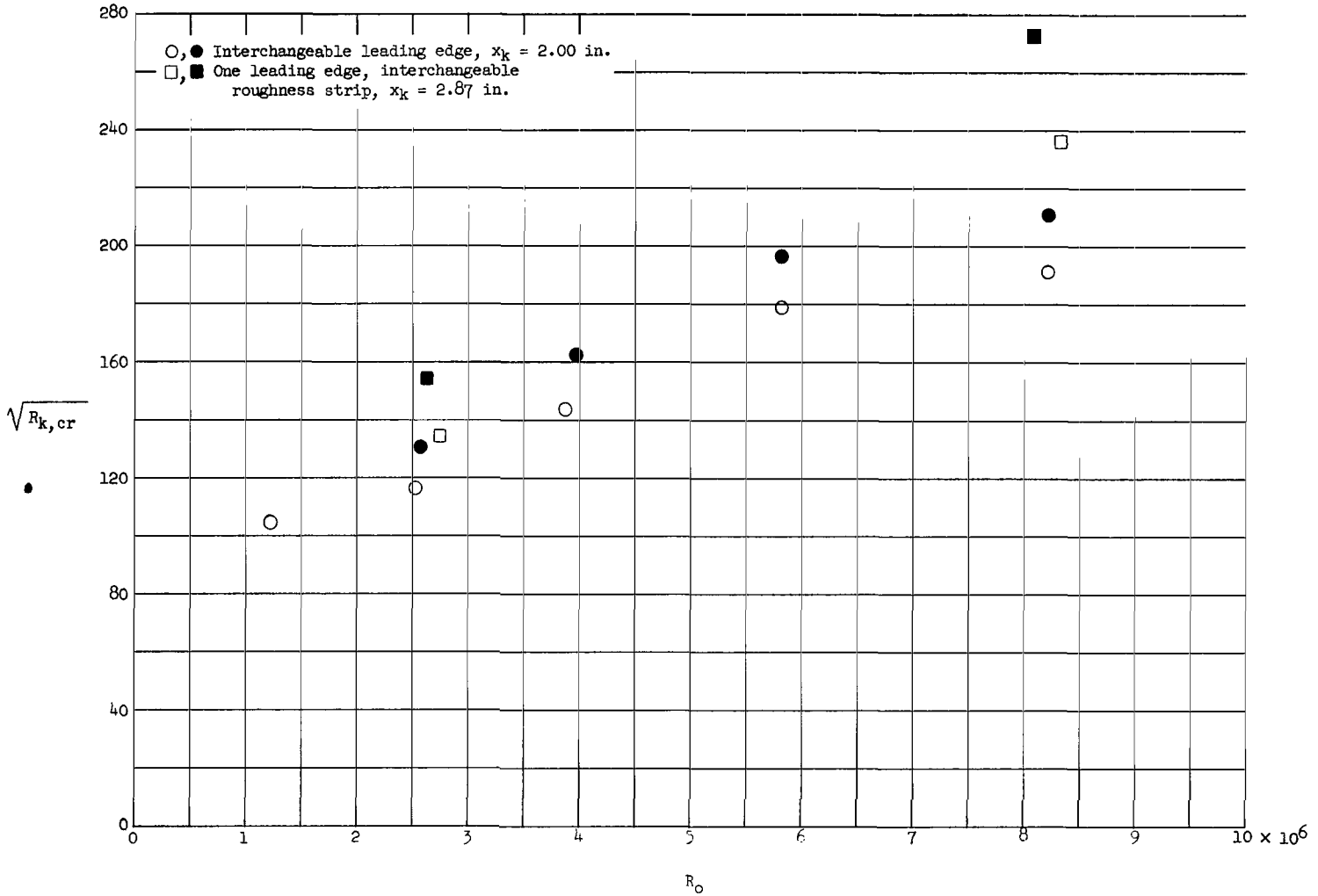

Figure 11.- Variation of critical roughness Reynolds number with free-stream unit Reynolds number for a Mach number of 6. (Open symbols indicate roughness height less than the critical value. Closed symbols indicate roughness height is slightly greater than the critical value.)

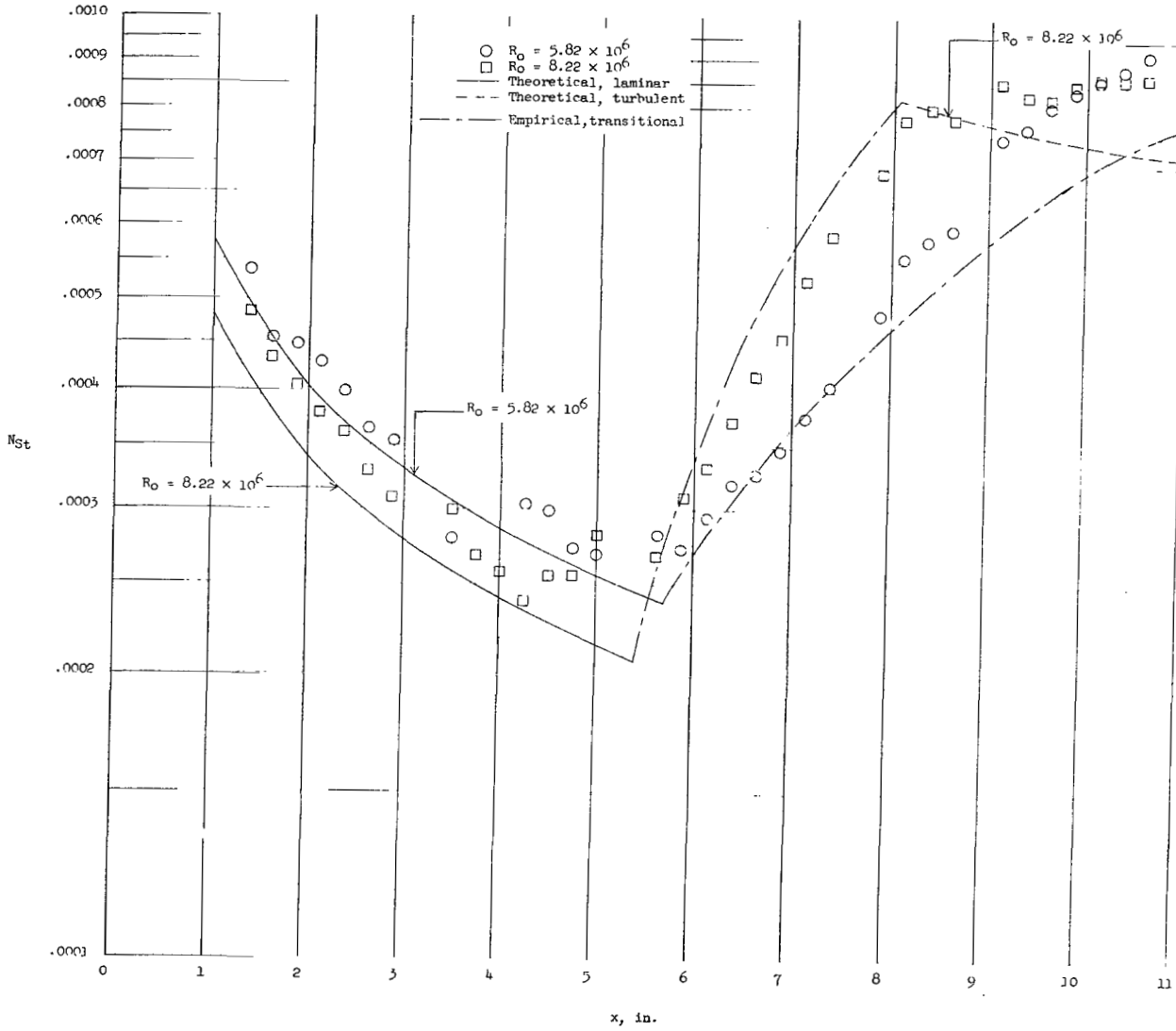

(a) $M_o = 6.0$.

Figure 12.- Heating-transfer distribution on continuous flat plate.

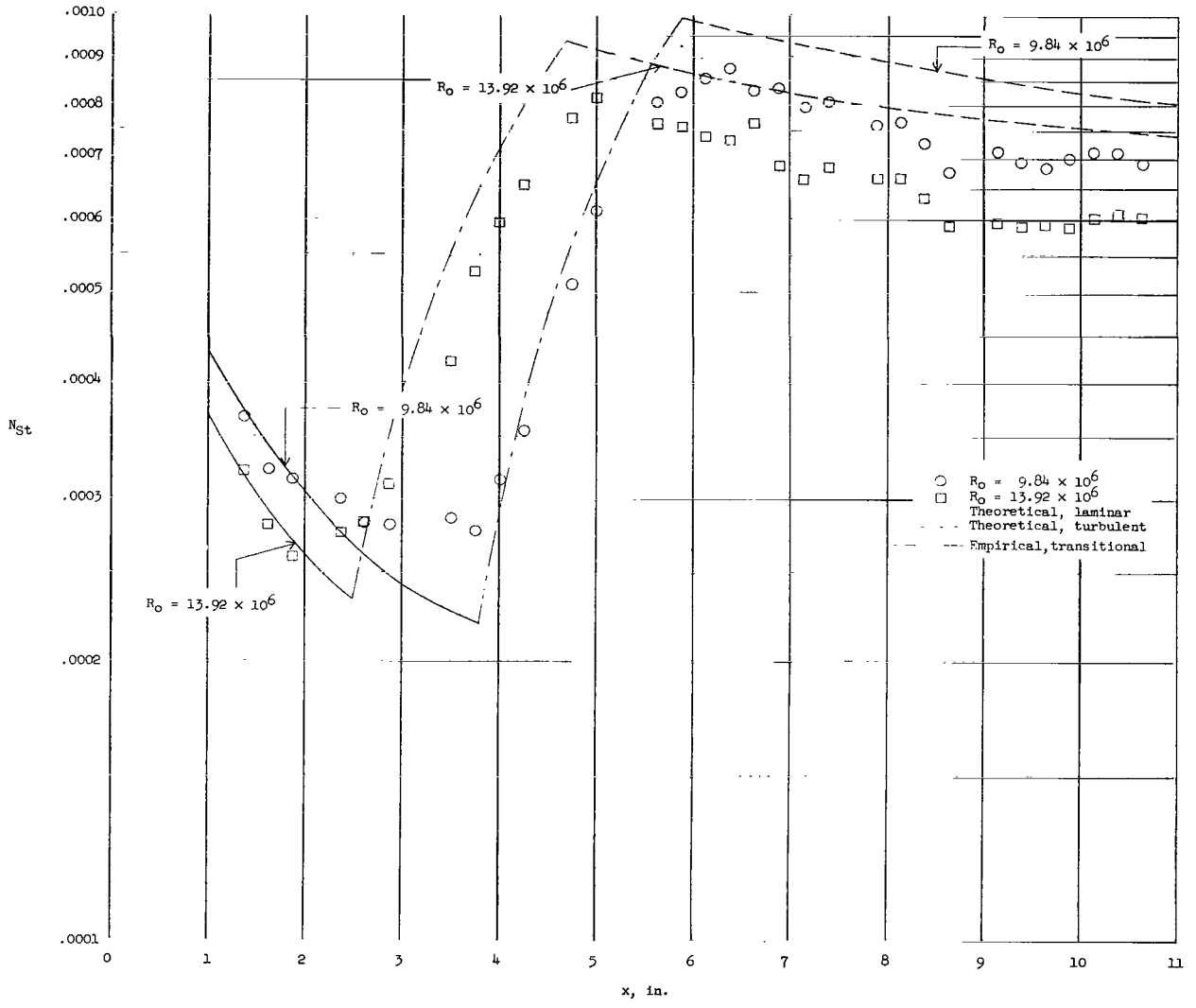

(b) M_o = 4.8.

Figure 12.- Concluded.

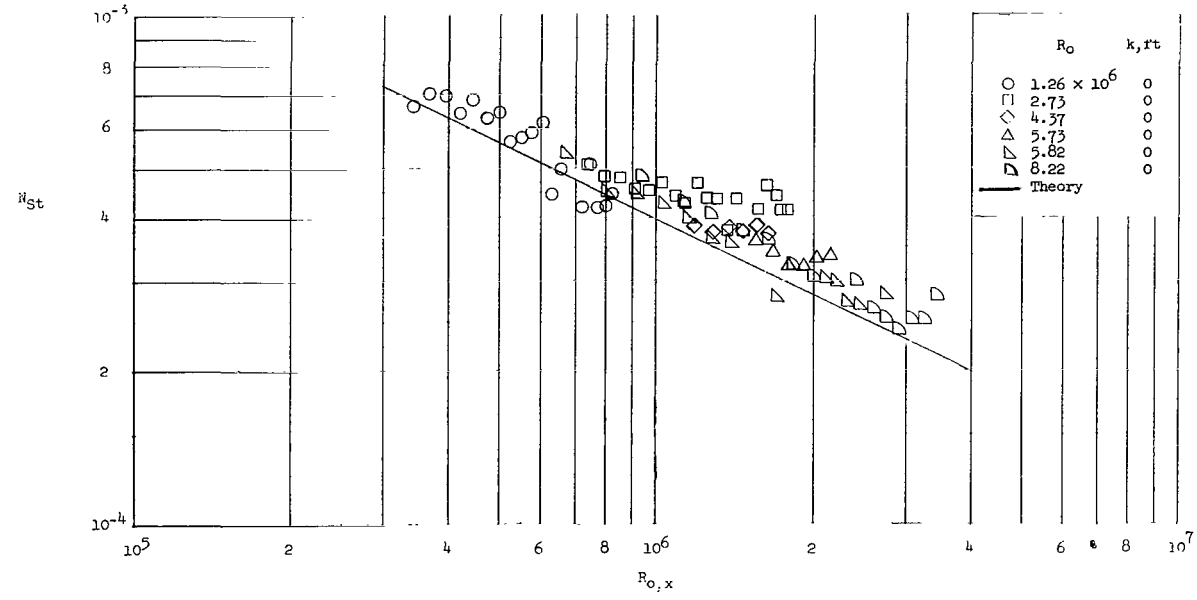

(a) $M_o = 6.0$.

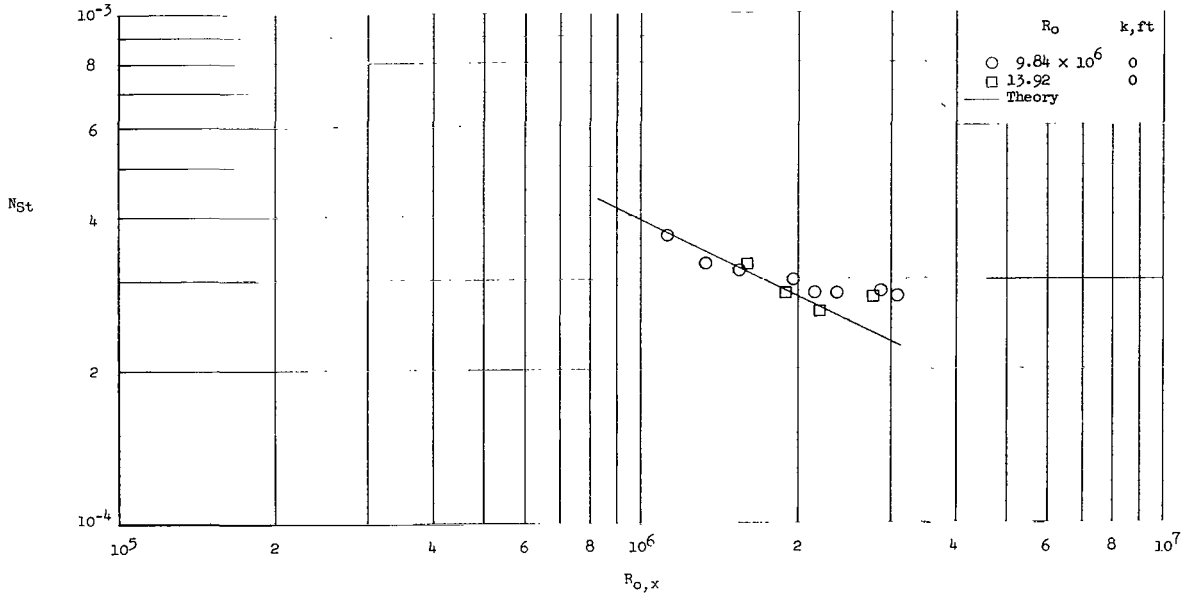

(b) $M_o = 4.8$.

Figure 13.- Comparison of laminar heat-transfer distributions as a function of local Reynolds number with theory.

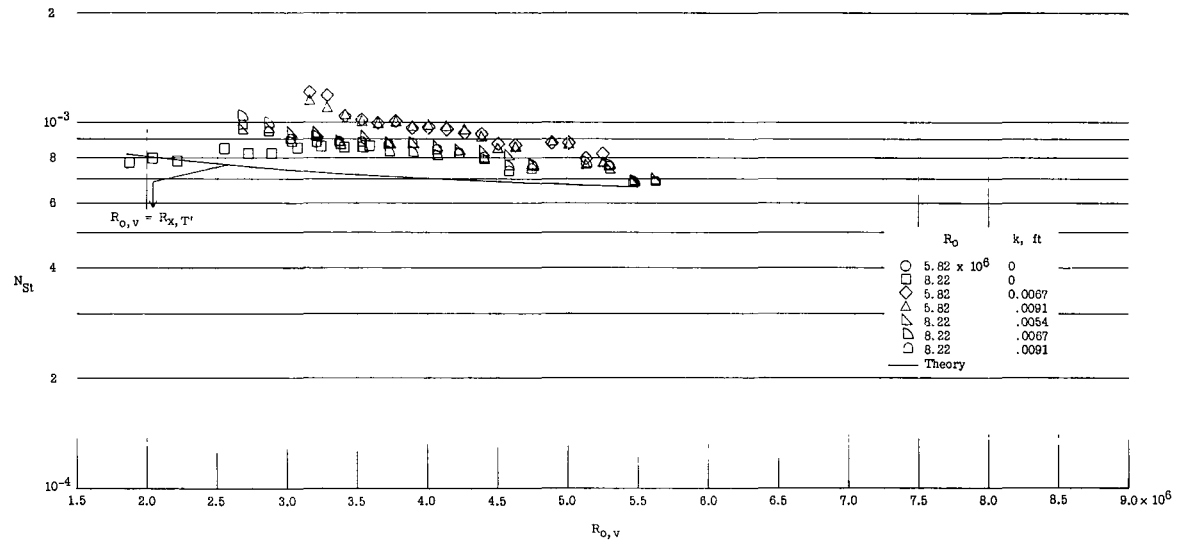

(a) $M_o = 6.0$.

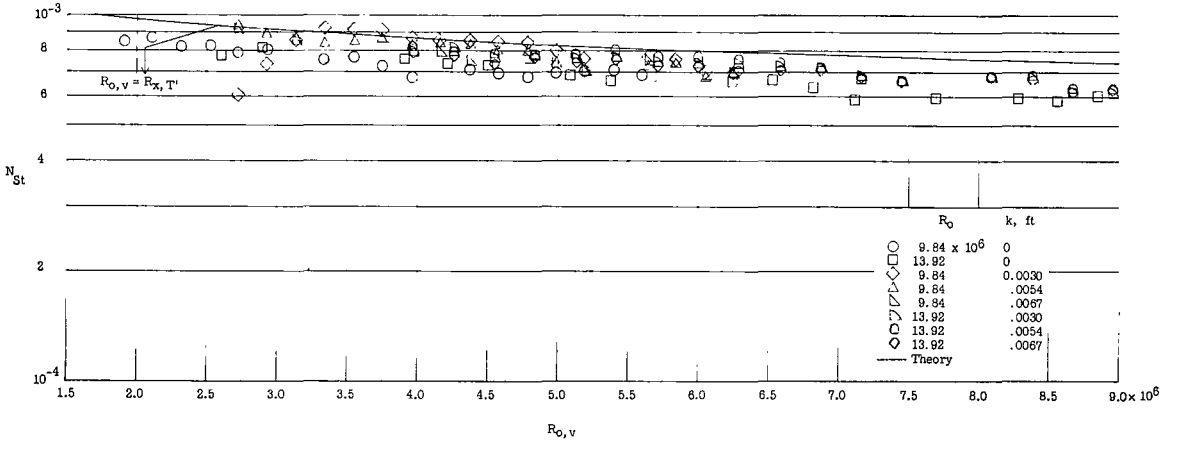

(b) $M_o = 4.8$.

Figure 14.- Comparison of turbulent heat-transfer distributions with theory for both natural transition and roughness.

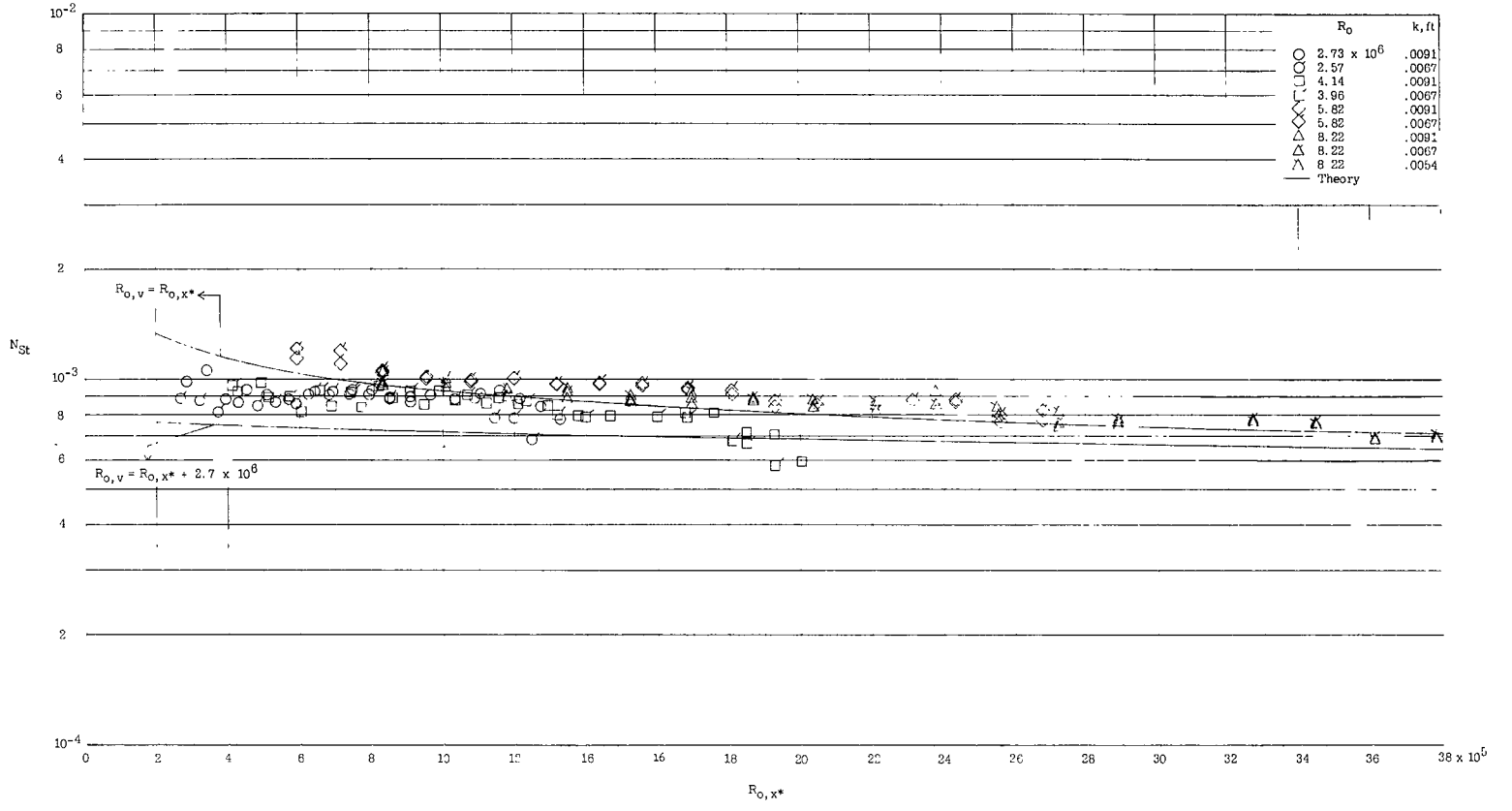

Figure 15.- Comparison of experimental turbulent heat-transfer distribution (with roughness) with distribution predicted by theory for complete test Reynolds number range.

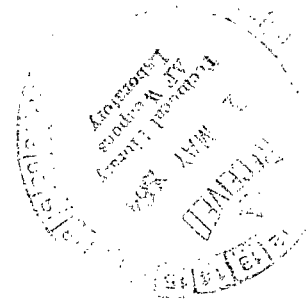

"The National Aeronautics and Space Administration . . . shall . . . provide for the widest practical appropriate dissemination of information concerning its activities and the results thereof . . . objectives being the expansion of human knowledge of phenomena in the atmosphere and space."

—National Aeronautics and Space Act of 1958

NASA SCIENTIFIC AND TECHNICAL PUBLICATIONS

TECHNICAL REPORTS: Scientific and technical information considered important, complete, and a lasting contribution to existing knowledge.

TECHNICAL NOTES: Information less broad in scope but nevertheless of importance as a contribution to existing knowledge.

TECHNICAL MEMORANDUMS: Information receiving limited distribution because of preliminary data, security classification, or other reasons.

CONTRACTOR REPORTS: Technical information generated in connection with a NASA contract or grant and released under NASA auspices.

TECHNICAL TRANSLATIONS: Information published in a foreign language considered to merit NASA distribution in English.

TECHNICAL REPRINTS: Information derived from NASA activities and initially published in the form of journal articles or meeting papers.

SPECIAL PUBLICATIONS: Information derived from or of value to NASA activities but not necessarily reporting the results of individual NASA-programmed scientific efforts. Publications include conference proceedings, monographs, data compilations, handbooks, sourcebooks, and special bibliographies.

Details on the availability of these publications may be obtained from:

SCIENTIFIC AND TECHNICAL INFORMATION DIVISION

NATIONAL AERONAUTICS AND SPACE ADMINISTRATION

Washington, D.C. 20546